

# **PERFORMANCE ANALYSIS OF FAST CELL SEARCH ALGORITHMS FOR W-CDMA SYSTEMS**

by

**JIAN LAWRENCE CHEN**

B. Eng., University of Victoria, 1999

**A THESIS SUBMITTED IN PARTIAL FULFILLMENT OF**

**THE REQUIREMENTS FOR THE DEGREE OF**

**MASTER OF APPLIED SCIENCE**

in

**THE FACULTY OF GRADUATE STUDIES**

**DEPARTMENT OF ELECTRICAL AND COMPUTER ENGINEERING**

**We accept this thesis as conforming**

**to the required standard**

**THE UNIVERSITY OF BRITISH COLUMBIA**

**April 2002**

**© Jian Lawrence Chen, 2002**

In presenting this thesis in partial fulfilment of the requirements for an advanced degree at the University of British Columbia, I agree that the Library shall make it freely available for reference and study. I further agree that permission for extensive copying of this thesis for scholarly purposes may be granted by the head of my department or by his or her representatives. It is understood that copying or publication of this thesis for financial gain shall not be allowed without my written permission.

Department of Electrical and Computer Engineering  
The University of British Columbia  
Vancouver, Canada

Date April 6<sup>th</sup>, 2002

# Abstract

A 3-stage fast cell search algorithm is adopted by the 3rd Generation Partnership Project (3GPP) committee as the method for establishing initial synchronization between a base station and a mobile station. The probability of detection analyses for stage 1 using the accumulation slot synchronization technique and stage 3 for Rayleigh fading channels have been previously studied.

In this thesis, the probability of detection for stage 1 using the most frequent occurrence method is analyzed and the results are compared with the accumulation technique. It is found that the accumulation scheme outperforms the most frequent occurrence scheme. The stage 2 probability of detection is also analyzed. All three stages are then analyzed in Ricean fading. As expected, it is observed that the probability of detection for all three stages in Ricean fading is better than that under Rayleigh fading channel. A theoretical model for the mean cell search time is also introduced. The results show that the mean cell search time increases more rapidly for the independent fading channel than for the block fading channel as the channel condition degrades.

The performance of the fast cell search algorithm was also studied using simulation. The simulation results were obtained based on SPW<sup>TM</sup> 3GPP model. Simulation results for a vehicular speed of 3 km/h were found to closely match the theoretical results assuming block fading. Results obtained assuming independent fading were found to be significantly different from simulation results for high vehicular speeds, e.g. 120 km/h. This is primarily due to the fact that even at this speed, the fading for consecutive slots are quite correlated.

# Table of Contents

<b>Abstract</b>	<b>ii</b>
<b>Table of Contents</b>	<b>iii</b>
<b>List of Figures</b>	<b>vii</b>
<b>Acknowledgment</b>	<b>viii</b>
<b>Dedication</b>	<b>ix</b>
<b>Chapter 1 Introduction</b>	<b>1</b>
1.1 Thesis Objectives and Organization.....	3
<b>Chapter 2 Background</b>	<b>5</b>
2.1 The Downlink Channel .....	5
2.1.1 The Frame Structure .....	6
2.1.2 The Downlink Transmission Structure .....	7
2.2 Channelization, Synchronization and Scrambling Codes.....	9
2.2.1 Channelization Codes .....	9
2.2.2 Scrambling Codes .....	10
2.2.3 Synchronization Codes .....	12
2.3 Previous Work on Theoretical Analysis of the Cell Search Algorithm .....	14
2.3.1 Stage 1.....	15
2.3.1.1 Independent Rayleigh Fading Model.....	19
2.3.1.2 Block Rayleigh Fading Model .....	19
2.3.2 Stage 2.....	20
2.3.3 Stage 3.....	21
<b>Chapter 3 Analysis of the 3-stage Cell Search Algorithm</b>	<b>24</b>

3.1	Stage 1 Analysis.....	24
3.1.1	Independent Rayleigh Fading Model.....	24
3.1.1.1	Accumulation Slot Synchronization Technique .....	24
3.1.1.2	Most Frequent Occurrence Slot Synchronization Technique .....	25
3.1.2	Block Rayleigh Fading Model .....	26
3.1.2.1	Accumulation Slot Synchronization Technique .....	26
3.1.2.2	Most Frequent Occurrence Slot Synchronization Technique .....	27
3.1.3	Independent Ricean Fading Model .....	28
3.1.3.1	Accumulation Slot Synchronization Technique .....	29
3.1.3.2	Most Frequent Occurrence Slot Synchronization Technique .....	29
3.1.4	Block Ricean Fading Model .....	29
3.1.4.1	Accumulation Slot Synchronization Technique .....	30
3.1.4.2	Most Frequent Occurrence Slot Synchronization Technique .....	30
3.2	Stage 2 Analysis.....	31
3.2.1	Independent Rayleigh Fading .....	32
3.2.2	Block Rayleigh Fading Model .....	34
3.2.3	Independent Ricean Fading Model .....	34
3.2.4	Block Ricean Fading Model .....	35
3.3	Stage 3 Analysis.....	36
3.3.1	Rayleigh Fading Model.....	36
3.3.2	Ricean Fading Model.....	36
3.4	Mean Synchronization Time.....	37
3.4.1	Independent fading.....	38

3.4.2 Block Fading .....	39
<b>Chapter 4 Results</b>	<b>42</b>
4.1 The SPW <sup>TM</sup> Simulation Model .....	42
4.1.1 System Level Parameters .....	42
4.1.2 The Description of SPW <sup>TM</sup> System Model .....	43
4.1.2.1 The 3GPP Base Station .....	44
4.1.2.2 Channel .....	45
4.1.2.3 Complex White Noise .....	45
4.1.2.4 Complex FIR Filter .....	45
4.1.2.5 Slot Synchronization .....	45
4.1.2.6 Code Group Identification and Frame Synchronization .....	46
4.1.2.7 Long Scrambling Code Identification .....	46
4.2 Stage 1 Results .....	47
4.2.1 Rayleigh Fading Model .....	47
4.2.2 Ricean Fading Model .....	50
4.3 Stage 2 Results .....	53
4.3.1 Rayleigh Fading Model .....	53
4.3.2 Ricean Fading Model .....	54
4.4 Stage 3 Results .....	55
4.4.1 Rayleigh Fading Model .....	55
4.4.2 Ricean Fading Model .....	56
4.5 Mean Cell Search Time .....	57
4.5.1 Rayleigh Fading Channel .....	57

4.5.2 Ricean Fading Channel .....	60
<b>Chapter 5 Conclusion</b>	<b>62</b>
5.1 Main Contributions of the Thesis .....	62
5.2 Future Work .....	63
<b>Glossary</b>	<b>65</b>
<b>References</b>	<b>72</b>
<b>Appendix A Allocation of SSCs for secondary SCH [10]</b>	<b>74</b>

## List of Figures

Figure 1.1	Roadmap to 3G systems [2].....	2
Figure 2.1	The frame structure definition as relevant to the cell search algorithm .....	6
Figure 2.2	The transmit processing of the P-CCPCH and SCH channels [9] .....	7
Figure 2.3	The combining of the 3 channels used in the cell search algorithm .....	9
Figure 2.4	Code tree for the OVSF codes [10].....	9
Figure 2.5	Three stage fast cell search algorithm.....	15
Figure 2.6	Slot synchronization.....	16
Figure 2.7	Code group identification and frame synchronization .....	21
Figure 2.8	Long scrambling code identification.....	22
Figure 4.1	The SPW <sup>TM</sup> fast cell search system model .....	43
Figure 4.2	Stage 1 performance under independent Rayleigh fading channel.....	48
Figure 4.3	Stage 1 performance under block Rayleigh fading channel .....	50
Figure 4.4	Stage 1 performance under independent Ricean fading channel .....	51
Figure 4.5	Stage 1 performance under block Ricean fading channel.....	52
Figure 4.6	Stage 2 performance under Rayleigh fading channel .....	54
Figure 4.7	Stage 2 performance under Ricean fading channel.....	55
Figure 4.8	Stage 3 performance under Rayleigh fading channel .....	56
Figure 4.9	Stage 3 performance under Ricean fading channel.....	57
Figure 4.10	Mean cell search time under independent Rayleigh fading channel.....	58
Figure 4.11	Mean cell search time under block Rayleigh channel .....	59
Figure 4.12	Mean cell search time under independent Ricean channel .....	60
Figure 4.13	Mean cell search time under block Ricean channel.....	61



## **Acknowledgment**

I would like to take this opportunity to express my sincere thanks and deep gratitude to my thesis advisor, Dr. Cyril Leung, for his guidance and encouragement. His critical reviews and many constructive suggestions were very essential to the completion of this work. This work was supported by an NSERC postgraduate scholarship, NSERC Grant OGP0001731 and a grant from Cadence Design Systems, Inc.

Friends and fellow students have certainly made my studies here a memorable and interesting one. I would like to thank Ms. Xiaoyan Feng, Mr. Vaibhav Dinesh, Mr. Xinrong Wang, Mr. Cyril Iskander, and other people in the Communications Group for their support and help.

Finally I would like to thank my parents, Mr. Dezhen Chen and Mrs. Huifang Zhang, my brother, Mr. Kang Chen, for their constant love and encouragement. They, too, have played a significant role in the completion of this work.

*To My Parents*

## Chapter 1 Introduction

In recent years there has been an explosive growth in the mobile communications market worldwide. In order to meet the increasing demand for higher data rate service and better spectrum efficiency, third generation (3G) mobile radio systems have been developed.

The initial impetus behind the development of 3G systems originated in Japan where the potential capacity of the current Personal Digital Cellular (PDC) system was seen to be a limit on the future growth of mobile communications. The Wideband Code Division Multiple Access (W-CDMA) system proposed by NTT DoCoMo as a replacement for the Japanese PDC system was recognized as a major improvement over GSM (Global System for Mobile communications) for greatly improved capacity and increased data services [1]. Subsequently, a number of proposals were submitted in response to the ITU's (International Telecommunication Union) IMT-2000 (International Mobile Telecommunications) initiative for the establishment of global standards for high speed wireless data transmission. However, the attempt to harmonize all proposals in a single 3G wireless mobile standard for the whole world was not successful.

It is anticipated that most GSM operators in Europe, Korea and Japan will migrate to W-CDMA either directly or through GPRS (General Packet Radio Service) or EDGE (Enhanced Data rate for GSM Evolution) and existing IS-95 operators in North America, Korea and Japan will migrate to CDMA2000. Figure 1.1 shows the road map from second to third generation mobile wireless systems [2].

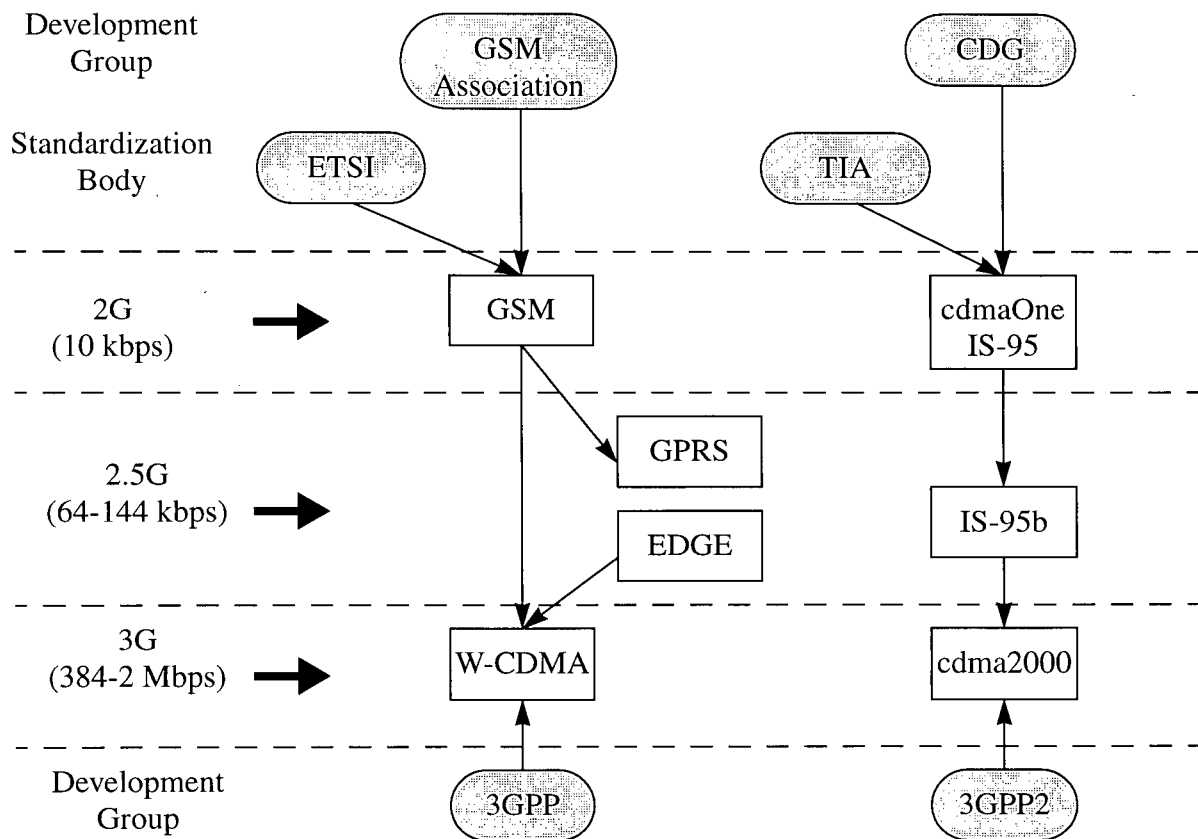


Figure 1.1 Roadmap to 3G systems [2]

One of the major differences between the W-CDMA and cdma2000 systems is that the CDMA2000 system is GPS (Global Positioning System) synchronized while W-CDMA is self synchronized [3]. Asynchronous cell site operation in W-CDMA does not require an external timing source. This means, for example, that there is no requirement that each base station be capable of reliable GPS reception. This will significantly reduce the deployment efforts, especially in indoor environment. To achieve continuous system deployment, a set of short orthogonal codes and cell-site-specific scrambling codes are used in the forward link. A mobile station (MS) must quickly establish forward-link scrambling code synchronization and measure the average received signal power of the best cell site (i.e., the site with the least propagation path

loss) at the beginning of communication. This process is called “cell search”[4].

Several hundred scrambling codes may be required in asynchronous cell operation. In general, the use of different scrambling codes at different cell sites increases the cell search time compared to single scrambling code usage, which can be applied to synchronous cell site systems such as in IS-95 [4]. To reduce the cell search time in asynchronous cell site operation, a number of fast cell search algorithms have been proposed [5],[6],[7],[8]. The 3-stage cell search method introduced in [5] was adopted in the third generation partnership project (3GPP) standard. Subsequently, the original cell search method was refined in the standardization process.

## 1.1 Thesis Objectives and Organization

In order to determine design parameters of the cell search algorithm, many combinations of the parameters need to be evaluated which usually requires tedious computer simulation. On the other hand, theoretical analysis reduces the burden of computer simulation and provides an estimation of the average cell search time.

The objective of this thesis is to provide a theoretical model of the 3-stage fast cell search algorithm. Two channel models, Rayleigh and Ricean, are considered in this thesis. Under each fading channel, two idealized conditions are assumed: independent fading and block fading. The definition for each case is given later in Chapter 3. To validate the theoretical model, simulations are performed and results are compared with those from the theoretical analysis.

More precisely, the objectives of this work are as follows:

- 1) To provide a theoretical model for each of the 3 stages of the fast cell search algorithm under independent and block Rayleigh and Ricean fading channels.

- 2) To produce an analytical estimate of the average cell search time under different fading conditions.
- 3) To present simulation work to validate the results obtained from the theoretical model.

The rest of this thesis is organized as follows. In Chapter 2, background information related to the fast cell search algorithm which includes downlink channel definition, frame structure, downlink transmission structure, and channelization and scrambling code definition is provided. A detailed description of the 3-stage fast cell search algorithm adopted by 3GPP is also provided in Chapter 2 followed by a review of related theoretical analyses of the cell search algorithm found in the literature.

In Chapter 3, a complete theoretical model of the 3-stage cell search algorithm is provided. The 3 stages are first analyzed individually to produce the probability of detection under Rayleigh and Ricean fading models. Then, an estimate of the average cell search time is given based on the probability of detection results obtained from the individual stages.

In Chapter 4, the simulation model using SPW<sup>TM</sup> (Signal Processing WorkSystem) is introduced and the simulation results are compared with the theoretical results. Finally, a summary of the main results of this thesis and some suggestions for possible future work are presented in Chapter 5.

## Chapter 2 Background

In order to understand the fast cell search algorithm, it is important to be first familiar with the frame structure and transmission formats for the various downlink channels in W-CDMA. In this chapter, the downlink channels used in cell search are introduced followed by detailed illustration of the frame structure and the downlink transmission structure. Following the downlink channel description, a thorough description of the generation and implementation of channelization, synchronization, and scrambling codes is also given in this chapter. The 3-stage cell search algorithm is then introduced, followed by a review of theoretical analysis of the cell search algorithm found in the literature.

### 2.1 The Downlink Channel

The W-CDMA downlink transmissions are carried over 5 MHz sub-channels. The transmissions from all the logical channels within a sub-channel are code division multiplexed and transmitted over the same physical channel occupying a 5 MHz band [9].

The following downlink physical channels are used for the cell search:

- Primary and Secondary Synchronization Channels (P-SCH and S-SCH).
- Common Pilot Channel (CPICH).
- Primary Common Control Physical Channel (P-CCPCH).

The P-CCPCH is a 30 kbps channel with a spreading factor of 256. The first symbol (256 chips) within a P-CCPCH slot is not transmitted. The P-CCPCH is continuously broadcast over the entire cell at a constant power level. All base stations use the same channelization code for P-CCPCH. However, the scrambling codes are different in the neighboring base stations.

The P-SCH and S-SCH are broadcast over the entire cell at a constant power level. Both these channels are transmitted only during the first 256 chips of a slot, when the P-CCPCH is not transmitted.

The Primary and Secondary SCH are not scrambled. The P-SCH is spread by the same code in every cell. However, the channelization code for the S-SCH depends on the group to which the scrambling code for that cell belongs. There are 64 possible code groups and hence 64 possible channelization codes for S-SCH.

### 2.1.1 The Frame Structure

In order to define the downlink channel transmission formats for the P-CCPCH, P-SCH, and S-SCH, a 10 ms frame is considered. The frame structure relevant to the cell search algorithm is shown in Figure 2.1. Each frame has 15 slots, each of which is  $2/3$  ms long. The symbol rate for the three channels is 15 ksym/s. Therefore, there are 150 symbols per frame and 10 symbols per slot. The spreading factor for these channels is 256. Therefore, every symbol has 256 chips.

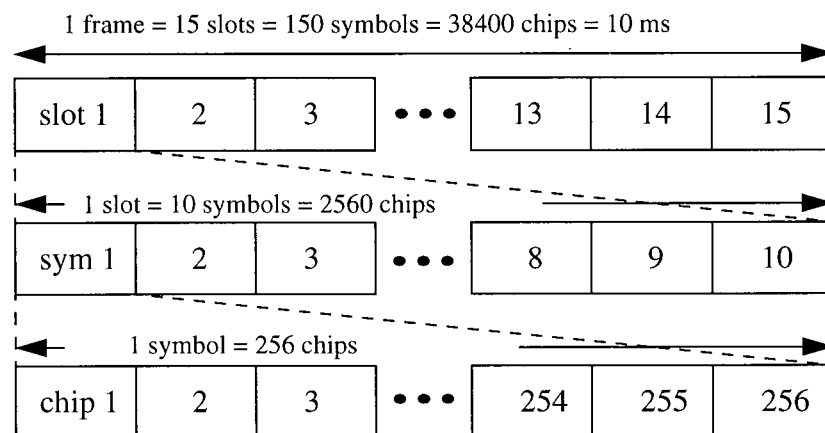


Figure 2.1 The frame structure definition as relevant to the cell search algorithm



### 2.1.2 The Downlink Transmission Structure

Control information is continually broadcast from all the base stations on the P-CCPCH, P-SCH and S-SCH. Figure 2.2 shows the downlink transmit processing for the three channels during a 10 ms frame. The processing shown is repeated every 10 ms. The processing shown in the figure does not reflect the actual implementation and is shown only to illustrate the resulting number of chips generated in each frame.

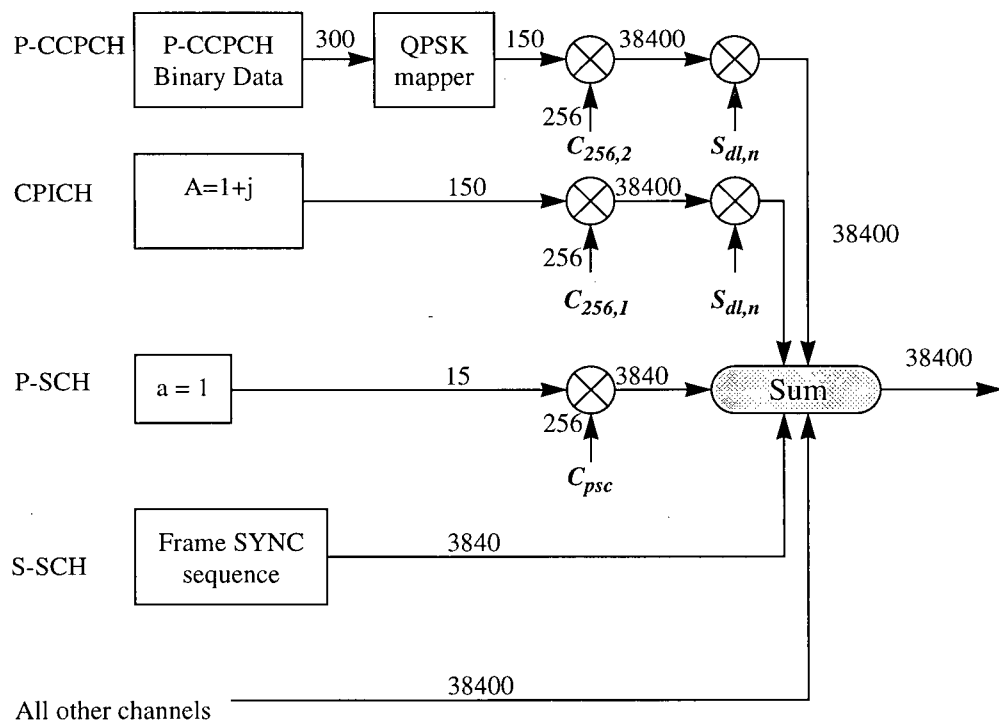


Figure 2.2 The transmit processing of the P-CCPCH and SCH channels [9]

The P-CCPCH carries 30 kbps of information. The bits are QPSK (Quadrature Phase Shift Keying) modulated. As far as the synchronization algorithms are concerned, the information content of these bits is irrelevant. In a 10 ms frame, 150 QPSK symbols are transmitted. The QPSK symbols are first spread using the OVSF (Orthogonal Variable Spreading Factor) code

$C_{256,2}$  of length 256 to produce 38400 chips. The resulting chips are scrambled by the primary scrambling code,  $S_{dl,n}$ , of length 38400 assigned to the cell are then combined with the chips from the other channels.

The CPICH continuously transmits the pilot symbol A at a rate of 15 ksym/s. The pilot symbols are spread with the  $C_{256,1}$  OVSF code and scrambled by the primary scrambling code  $S_{dl,n}$ .

The P-SCH transmits the same synchronization symbol in every slot of a given frame. This may be represented by a symbol spread by a short code  $C_{psc}$  of length 256 to produce 256 chips per slot transmitted at the beginning of each slot.

There are 64 possible code groups to which a base station can belong. The code group determines which scrambling codes may be used by that base station. The S-SCH indicates the code group to which the base belongs. To accomplish this, one of 64 possible synchronization sequences of length 3840, also known as the Frame SYNC sequence, are transmitted on the S-SCH repeatedly. The sequence is composed of a sequence of 15 codes, each chosen from a set of 16 possible Secondary Synchronization Codes (SSC), each SSC is 256 chips long.

The combining of the three channels is shown in Figure 2.3. The S-SCH and P-SCH transmit only 1 symbol (256 chips) at the beginning of each slot (symbol 1 in every slot). The transmitted waveform is the sum of the signals transmitted in parallel.

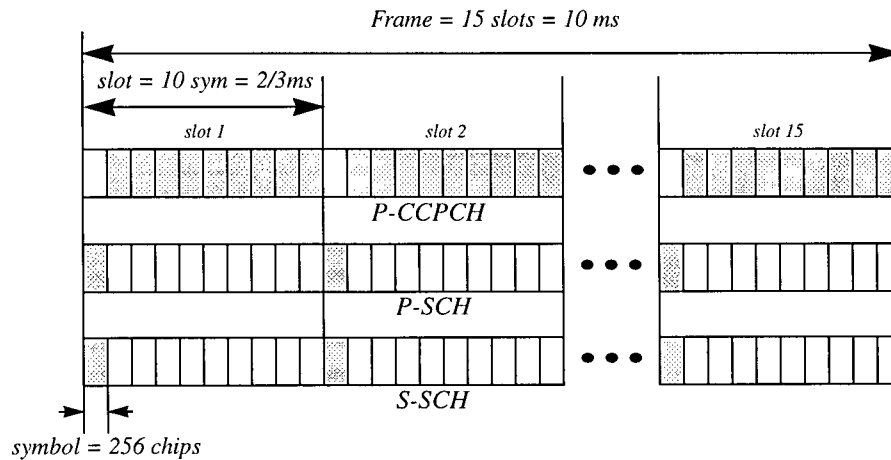


Figure 2.3 The combining of the 3 channels used in the cell search algorithm

## 2.2 Channelization, Synchronization and Scrambling Codes

### 2.2.1 Channelization Codes

The OVSF codes are used to preserve the orthogonality between downlink channels of different rates and spreading factors. The OVSF codes are defined in Figure 2.4.

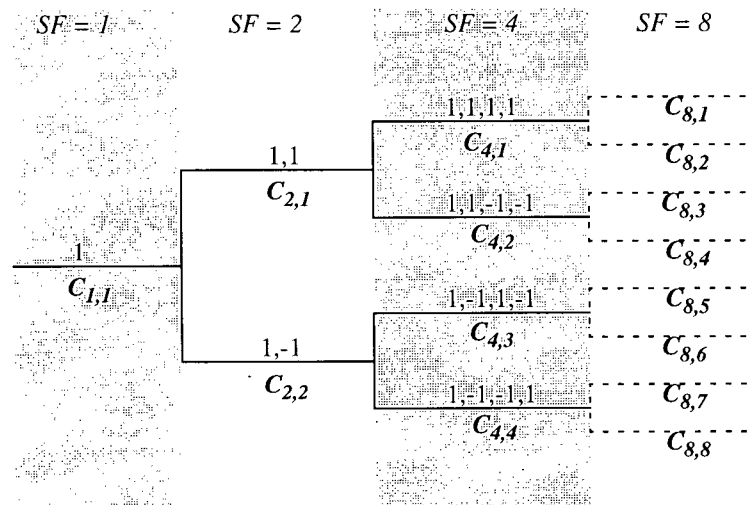


Figure 2.4 Code tree for the OVSF codes [10]

The channelization code for the CPICH is fixed to  $C_{256,1}$  and the channelization code for the P-CCPCH is fixed to  $C_{256,2}$ . The channelization codes for all other physical channels are assigned by UTRAN (Universal Terrestrial Radio Access Network).

### 2.2.2 Scrambling Codes

A total of  $2^{18} - 1 = 262143$  scrambling codes, numbered 0, ..., 262142 can be generated. However not all the scrambling codes are used. The scrambling codes are divided into 512 sets, each consisting of a primary scrambling code and 15 secondary scrambling codes.

The primary scrambling codes consist of scrambling codes  $n = 16 \times i$  where  $i = 0, \dots, 511$ . The  $i^{th}$  set of secondary scrambling code consists of scrambling codes  $16 \times i + k$ , where  $k = 1, \dots, 15$ .

Hence, according to the above, scrambling codes  $k = 0, 1, \dots, 8191$  are used. The set of primary scrambling codes is further divided into 64 scrambling code groups, each consisting of 8 primary scrambling codes. The  $j^{th}$  scrambling code group consists of primary scrambling codes  $16 \times 8 \times j + 16 \times k$ , where  $j = 0, \dots, 63$  and  $k = 0, \dots, 7$ .

Each cell is allocated one and only one primary scrambling code. The CCPCH and P-CPICH are always transmitted using the primary scrambling code. The other downlink physical channels can be transmitted with either the primary scrambling code or a secondary scrambling code from the set associated with the primary scrambling code of the cell.

The scrambling code sequences are constructed by combining two real sequences into a

complex sequence. Each of the two real sequences is constructed as the position wise modulo 2 sum of 38400 chip segments of two binary m-sequences generated by means of two generator polynomials of degree 18. The resulting sequences thus constitute segments of a set of Gold sequences [10]. The scrambling codes are repeated for every 10 ms frame. Let  $x$  and  $y$  be the two sequences respectively. The  $x$  sequence is constructed using the primitive (over GF(2)) polynomial  $1 + x^7 + x^{18}$ . The  $y$  sequence is constructed using the primitive polynomial  $1 + x^5 + x^7 + x^{10} + x^{18}$ .

Let the sequence corresponding to the chosen scrambling code number  $n$  be denoted by  $z_n$ . Furthermore, let  $x(i)$ ,  $y(i)$  and  $z_n(i)$  denote the  $i^{th}$  symbol of the sequences  $x$ ,  $y$ , and  $z_n$ , respectively.

The m-sequences  $x$  and  $y$  are constructed as follows

$$x(i + 18) = x(i + 7) + x(i) \text{ modulo } 2, \quad i = 0, \dots, 2^{18} - 20,$$

$$y(i + 18) = y(i + 10) + y(i + 7) + y(i + 5) + y(i) \text{ modulo } 2, \quad i = 0, \dots, 2^{18} - 20$$

with initial conditions

$$x(0) = 1, x(1) = x(2) = \dots = x(16) = x(17) = 0,$$

$$y(0) = 1, y(1) = y(2) = \dots = y(16) = y(17) = 1.$$

The  $n^{th}$  Gold code sequence  $z_n$ ,  $n = 0, 1, 2, \dots, 2^{18} - 2$ , is then defined as

$$z_n(i) = x((i + n) \text{ modulo } (2^{18} - 1)) + y(i) \text{ modulo } 2, \quad i = 0, \dots, 2^{18} - 2.$$

These binary sequences are converted to real valued sequences  $Z_n$  by the following transformation

$$Z_n(i) = \begin{cases} 1 & \text{if } z_n(i) = 0 \\ -1 & \text{if } z_n(i) = 1 \end{cases} \quad \text{for } i = 0, \dots, 2^{18} - 2.$$

Finally, the  $n^{th}$  complex scrambling code sequence  $S_{dl,n}$  is defined as

$$S_{dl,n}(i) = Z_n(i) + jZ_n((i + 131072) \text{ modulo } (2^{18} - 1)) \quad i = 0, 1, \dots, 38399.$$

Note that the pattern from phase 0 up to phase 38399 is repeated [10].

### 2.2.3 Synchronization Codes

The Primary Synchronization Code (PSC),  $C_{psc}$  is constructed as a so-called generalized hierarchical Golay sequence [10]. The PSC is furthermore chosen to have good aperiodic auto correlation properties.

Define

$$\mathbf{a} = (x_1, x_2, x_3, \dots, x_{16}) = (1, 1, 1, 1, 1, 1, -1, -1, 1, -1, 1, -1, 1, -1, -1, 1).$$

The PSC is generated by repeating the sequence modulated by a Golay complementary sequence,

and creating a complex-valued sequence with identical real and imaginary components. The PSC

$C_{psc}$  is defined as

$$C_{psc} = (1 + j) \times (a, a, a, -a, -a, a, -a, -a, a, a, a, -a, a, -a, a, a),$$

where the leftmost chip in the sequence corresponds to the chip transmitted first in time.

The 16 Secondary Synchronization Codes (SSCs),  $(C_{ssc, 1}, \dots, C_{ssc, 16})$ , are complex-valued with identical real and imaginary components, and are constructed from position wise multiplications of a Hadamard sequence and a sequence  $z$ , defined as

$$z = (b, b, b, -b, b, b, -b, -b, b, -b, b, -b, -b, -b, -b, -b),$$

where  $\mathbf{b} = (x_1, x_2, x_3, x_4, x_5, x_6, x_7, x_8, -x_9, -x_{10}, -x_{11}, -x_{12}, -x_{13}, -x_{14}, -x_{15}, -x_{16})$  and

$x_1, x_2, x_3, \dots, x_{16}$  are same as in the definition of the sequence  $\mathbf{a}$  above.

The Hadamard sequences are obtained as the rows in a matrix  $\mathbf{H}_8$  constructed recursively by

$$\mathbf{H}_0 = (1),$$

$$\mathbf{H}_k = \begin{bmatrix} \mathbf{H}_{k-1} & \mathbf{H}_{k-1} \\ \mathbf{H}_{k-1} & -\mathbf{H}_{k-1} \end{bmatrix} \quad k \geq 1.$$

The rows are numbered from the top starting with row 0 (the all ones sequence). The sequence  $\mathbf{h}_n$

denotes the  $n^{th}$  Hadamard sequence as a row of  $\mathbf{H}_8$  numbered from the top,  $n = 0, 1, \dots, 255$ .

Furthermore, let  $h_n(i)$  and  $z(i)$  denote the  $i^{th}$  symbols of the sequences  $h_n$  and  $z$ , respectively, where  $i = 0, 1, \dots, 255$  and  $i = 0$  corresponds to the leftmost symbol.

The  $k^{th}$  SSC,  $C_{ssc,k}$ ,  $k = 1, 2, 3, \dots, 16$  is then defined as

$$C_{ssc,k} = (1 + j) \times (h_m(0) \times z(0), h_m(1) \times z(1), h_m(2) \times z(2), \dots, h_m(255) \times z(255));$$

where  $m = 16 \times (k - 1)$  and the leftmost chip in the sequence corresponds to the chip transmitted first in time.

The 64 Frame SYNC sequences are constructed such that their cyclic-shifts are unique, i.e., a non-zero cyclic shift less than 15 of any of the 64 sequences is not equivalent to some cyclic shift of any other of the 64 sequences. Also, a non-zero cyclic shift less than 15 of any of the sequences is not equivalent to itself. Appendix A describes the sequences of SSCs used to encode the 64 different scrambling code groups. The entries in Appendix A denote what SSC to use in the different slots for the different scrambling code groups, e.g. the entry “7” means that SSC  $C_{ssc,7}$  shall be used for the corresponding scrambling code group and slot.

### 2.3 Previous Work on Theoretical Analysis of the Cell Search Algorithm

The fast cell search algorithm [11] is performed in three stages as shown in Figure 2.5

- slot synchronization
- code-group identification and frame synchronization
- long scrambling code identification



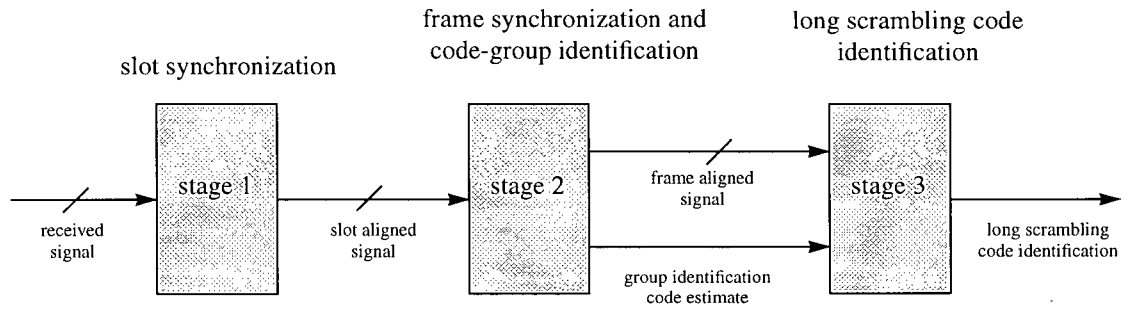


Figure 2.5 Three stage fast cell search algorithm

A number of papers have been published in the area of estimating the optimal design parameters and evaluating the performance of the fast cell search algorithm using simulations [12][13][14]. However, in this section, the focus is on work related to theoretical analysis of the fast cell search algorithm. A theoretical analysis for stage 1 implementing the accumulation method and stage 3 is proposed in [17].

### 2.3.1 Stage 1

The mobile station must select and synchronize to the base station from which it receives the best signal. As explained in Section 2.1.2, a sequence of length 256 is periodically transmitted on the P-SCH. This sequence is used for slot synchronization. The down converted and digitized baseband received signals are passed through a filter matched to the sequence  $C_{psc}$ . The output of the matched filter within the duration of a slot will have a peak corresponding to the slot boundary. In order to ensure a reliable selection, the output of the matched filter is observed over a number of consecutive slots. Two slot synchronization techniques are considered in this thesis. The first is the accumulation method in which the output of the filter is accumulated over a number of slot durations. The second is the most frequent occurrence method in which the output

of the matched filter is observed after each slot duration and the peak location is stored in a buffer. After  $N_1$  slots, the peak location which has occurred most frequently is chosen as the delay estimate that indicates the delay from the base station to the mobile. This delay is compensated for by the receiver. The operation for stage 1 is illustrated in Figure 2.6.

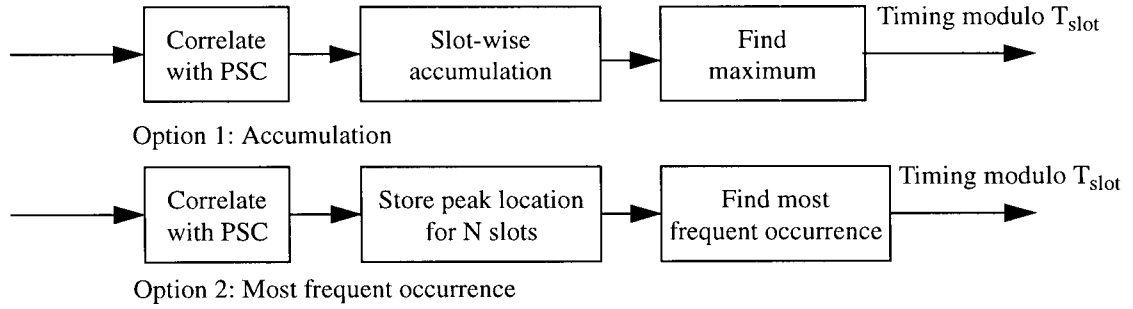


Figure 2.6 Slot synchronization

In slot synchronization, the number of slots used is a parameter which needs to be optimized. The larger this number is, the more the fading and noise are averaged, resulting in better performance for this stage. However, the time required for stage 1 completion will also increase.

If  $N_1$  slot durations are accumulated in stage 1, then, for each of the 2560 possible locations of PSC hypotheses, denoted by  $u$ ,  $0 \leq u \leq 2559$ , the result r.v. (random variable)  $Y_1(u)$  at the output of the correlator is defined as [17]

$$Y_1(u) = \sum_{i=0}^{N_1-1} \left| \sum_{j=0}^{255} y_{j+Ti+u} C_{PSC,j} \right|^2, \quad (2.1)$$

where  $y_i$  are the received complex signals, sampled at chip intervals, with  $y_0$  being the first sample received when stage 1 begins;  $C_{PSC, j}$  is the  $j^{th}$  real chip of the PSC, and  $T = 2560$  is the interval between successive  $C_{PSC}$  measured in chip intervals. It can be seen that  $y_i$  is made up of the signal component  $s_i$  and the noise component  $n_i$ . Substituting  $s_i$  and  $n_i$  for  $y_i$ , (2.1) can be written as

$$Y_1(u) = \sum_{i=0}^{N_1-1} \left| \sum_{j=0}^{255} s_{j+Ti+u} C_{PSC, j} + \sum_{j=0}^{255} n_{j+Ti+u} C_{PSC, j} \right|^2. \quad (2.2)$$

Without loss of generality, assuming that  $u = 0$  is the correct chip location and that when

$u \neq 0$ , the term  $\sum_{j=0}^{255} s_{j+Ti+u} C_{PSC, j}$  is equal to zero, (2.2) can be expressed as

$$Y_1(u) \cong \begin{cases} \sum_{i=0}^{N_1-1} |X_i + n_i^{(u)}|^2, & u = 0, & \text{correct hypothesis} \\ \sum_{i=0}^{N_1-1} |n_i^{(u)}|^2, & u \neq 0, & \text{incorrect hypothesis,} \end{cases} \quad (2.3)$$

where  $\{X_i, i = 0, 1, \dots, N_1 - 1\}$  are the signal components at the correlator output at the  $i$ th slot duration, and  $n_i^{(u)}$  is the background multiple access interference (MAI) plus noise, which, following [15], is modeled as a complex i.i.d. (independent identical distributed) Gaussian r.v. with zero mean and unit variance ( $n_i^{(u)} \sim N_c(0, 1)$ ).

The fading process is assumed constant over a symbol period but varies across symbols.

As a result,  $\{X_i, i = 0, 1, \dots, N_1 - 1\}$  are complex r.v.'s with variance  $E_{s,PSCH}/I_0$ , where  $E_{s,PSCH}$  is the average symbol energy for the P-SCH and  $I_0$  is the background noise plus MAI variance. The normalization by  $I_0$  takes into account the unit variance assumption of  $n_i^u$ .

For  $u \neq 0$ ,  $Y_1(u)$  is  $\chi^2$  distributed with  $2N_1$  degrees of freedom [16], i.e.

$$P[Y_1(u) > \tau | u \neq 0] = F_{N_1}(\tau) = e^{-\tau/2} \sum_{i=0}^{N_1-1} \frac{1}{i!} \left(\frac{\tau}{2}\right)^i, \quad (2.4)$$

where  $F_{N_1}(\tau)$  is the complementary Cumulative Distribution Function (CDF) of a  $\chi^2$  r.v. with  $2N_1$  degrees of freedom [16].

Let  $p_d^{(1)}$  be the probability of selecting the correct chip location as the estimate of the slot boundary and the superscript denotes the stage. Noting that  $Y_1(u)$  is independent, we get [17]

$$p_d^{(1)} = \int_0^{\infty} (1 - F_{N_1}(\tau))^{2559} f_{Y_1(0)}(\tau) d\tau, \quad (2.5)$$

where  $1 - F_{N_1}(\tau)$  is the probability that  $Y_1(u) \leq \tau$ ,  $u \neq 0$  and  $f_{Y_1(0)}(\tau)$  is the pdf (Probability Density Function) of  $Y_1(0)$ . The term  $(1 - F_{N_1}(\tau))^{2559}$  accounts for the fact that there are 2559 non-zero values of  $u$ , i.e.  $u = 1, 2, \dots, 2559$ .

The following two idealized channel conditions were considered to determine  $f_{Y_1(0)}(\tau)$  in [17].

### 2.3.1.1 Independent Rayleigh Fading Model

To model independent Rayleigh fading, we assume that the signal undergoes independent Rayleigh fading in successive slots, i.e.  $\{X_i, i = 0, 1, \dots, N_1 - 1\}$  are complex Gaussian i.i.d. Then  $(X_i + n_i'') \sim N_c(0, 1 + E_{s, PSCH}/I_0)$  and  $Y_1(0)$  is  $\chi^2$  distributed with  $2N_1$  degrees of freedom, and we get [16]

$$f_{Y_1(0)}(\tau) = \frac{\tau^{N_1-1} e^{-\tau/(2(1+E_{s, PSCH}/I_0))}}{(2(1+E_{s, PSCH}/I_0))^{N_1} (N_1-1)!}. \quad (2.6)$$

### 2.3.1.2 Block Rayleigh Fading Model

To model block Rayleigh fading, we assume that the fading is constant over  $N_1$  time slots (a block), i.e.  $X_i = X$  for  $0 \leq i \leq N_1 - 1$ , where  $X \sim N_c(0, E_{s, PSCH}/I_0)$ , changing from block to block. For any given block, given  $|X|^2 = x$ ,  $Y_1(0)$  is non-central  $\chi^2$  distributed with  $2N_1$  degrees of freedom and the conditional pdf  $f_{Y_1(0)|X|^2=x}(\tau)$  is given by [16]

$$f_{Y_1(0)|X|^2=x}(\tau) = \frac{1}{2} \left( \frac{\tau}{N_1 x} \right)^{\frac{N_1-1}{2}} e^{-\frac{(N_1 x + \tau)}{2}} I_{N_1-1}(\sqrt{N_1 \tau x}), \quad (2.7)$$

where  $I_{N_1-1}(x)$  is the  $(N_1 - 1)^{th}$  order modified Bessel function of the first kind. Since  $|X|^2$  is  $\chi^2$  distributed with 2 degrees of freedom, the pdf of  $Y_1(0)$  for the block fading model can be written as

$$f_{Y_1(0)}(\tau) = \int_0^{\infty} \frac{1}{2} \left( \frac{\tau}{N_1 x} \right)^{\frac{N_1-1}{2}} e^{-\frac{(N_1 x + \tau)}{2}} I_{N_1-1}(\sqrt{N_1 \tau x}) \frac{e^{-\frac{x}{2E_{s, PSCH}/I_0}}}{2E_{s, PSCH}/I_0} dx. \quad (2.8)$$

### 2.3.2 Stage 2

Having acquired slot timing, the MS has to find both the code group and the start of the frame. This is done by cross correlating the received sequence with the 16 possible  $C_{SSC}$  for 15 consecutive slots. At the end of the  $i^{th}$  slot, the SSC number that produces the largest correlation value is stored in the  $i^{th}$  position of a buffer called the code sequence. After 15 slots, the content of the code sequence buffer, which can take on  $15^{16} = 6.57 \times 10^{18}$  possible values, is compared with the 64 Frame SYNC sequences and all their distinct cyclic shifts and the Frame SYNC sequence with the corresponding shift that produces the minimum Hamming distance indicates the code group and the start of frame. The operation of stage 2 is illustrated in Figure 2.7. It is difficult to obtain probability of detection for stage 2 analytically; therefore, only simulation results exist for this stage in previously published literature.

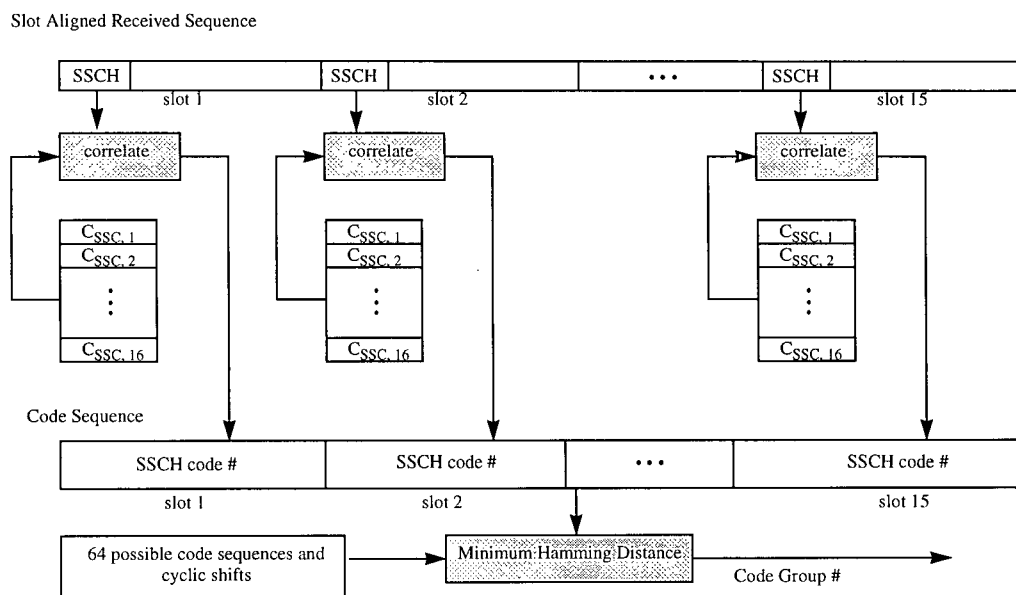


Figure 2.7 Code group identification and frame synchronization

### 2.3.3 Stage 3

Having acquired slot timing, frame synchronization, and the long code group, the mobile station has to search amongst the possible 8 scrambling codes within the code group to find the base station's scrambling code. This is accomplished through symbol by symbol correlation of the received sequence over CPICH (up to 38400 chips) with the 8 possible long sequences. The scrambling code sequence that produces the maximum correlation value is selected. The operation of stage 3 is illustrated in Figure 2.8.

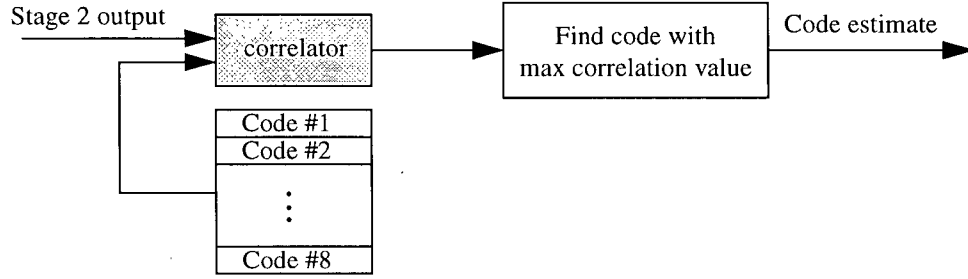


Figure 2.8 Long scrambling code identification

If there are 8 parallel correlators available in stage 3 and the number of slots used for correlation is 1, i.e.  $N_3 = 1$ , then the result r.v.  $Y_3(w)$  at the output of the correlator is defined as follows

$$Y_3(w) = \left| \sum_{j=0}^{2559} y_j S_{dl, w_j} \right|^2, \quad (2.9)$$

where  $y_i$  are the received slot and frame boundary aligned complex signals, sampled at chip intervals, with  $y_0$  being the first sample received when stage 3 begins;  $S_{dl, w}$  is the  $w^{th}$  scrambling code of the code group determined by stage 2. Without loss of generality, assuming that  $S_{dl, 0}$  is the correct scrambling code, (2.9) implies

$$Y_3(w) \equiv \begin{cases} |X + n_i^{(w)}|^2, & w = 0 & \text{correct hypothesis} \\ |n_i^{(w)}|^2, & w \neq 0 & \text{incorrect hypothesis,} \end{cases} \quad (2.10)$$

where  $0 \leq w \leq 7$  because there are 8 possible scrambling codes.

Let  $p_d^{(3)}$  be the probability of selecting the correct scrambling code. Following the



analysis of stage 1, we have [17]

$$\begin{aligned}
 p_d^{(3)} &= \int_0^\infty (1 - F_1(\tau))^7 f_{Y_3(0)}(\tau) d\tau = \int_0^\infty \left(1 - e^{-\frac{\tau}{2}}\right)^7 \frac{e^{-\frac{\tau}{2(1+E_{s,CPICH}/I_0)}}}{2(1+E_{s,CPICH}/I_0)} d\tau \\
 &= \frac{7!(1+E_{s,CPICH}/I_0)^7}{\prod_{i=1}^7 (1+i(1+E_{s,CPICH}/I_0))},
 \end{aligned} \tag{2.11}$$

where  $E_{s,CPICH}/I_0$  denotes the symbol energy to interference ratio for CPICH.

## Chapter 3 Analysis of the 3-stage Cell Search Algorithm

The probability of detection analysis for stage 1 using the accumulation method and stage 3 in Rayleigh fading was reviewed in Chapter 2. In this chapter, the probability of detection analysis for stage 1 using the most frequent occurrence method is introduced. An analysis of the probability of detection for stage 2 is also provided. Furthermore, the analyses for all three stages of the fast cell search algorithm under Ricean fading are described. A theoretical estimate of the overall average cell search time is also given.

### 3.1 Stage 1 Analysis

The details of stage 1 probability of detection analysis for the accumulation method in Rayleigh fading are provided in Chapter 2. In this section, the stage 1 analysis for the most frequent occurrence method is introduced. The analysis of stage 1 in Ricean fading is also introduced.

#### 3.1.1 Independent Rayleigh Fading Model

In this model, we assume that the signal undergoes independent Rayleigh fading in successive slots, i.e.  $\{X_i, i = 0, 1, \dots, N_1 - 1\}$  are i.i.d. complex Gaussian r.v.'s. Then

$$(X_i + n_i^u) \sim N_c(0, 1 + E_{s, PSCH}/I_0).$$

##### 3.1.1.1 Accumulation Slot Synchronization Technique

From (2.5), the probability of detection for stage 1 in independent Rayleigh fading is

$$p_d^{(1)} = \int_0^{\infty} (1 - F_{N_1}(\tau))^{2559} f_{Y_1(0)}(\tau) d\tau, \quad (3.1)$$

where  $F_{N_1}(\tau)$  is given by (2.4), and  $f_{Y_1(0)}(\tau)$  is given by (2.6).

### 3.1.1.2 Most Frequent Occurrence Slot Synchronization Technique

Instead of accumulating the output of the matched filter over  $N_1$  slot durations, we now store the peak location of the matched filter output after each slot duration and choose the most frequently occurring peak location after  $N_1$  slot durations as the slot boundary estimate.

In order to determine  $p_d^{(1)}$ , we first need to consider the probability of detection when only one slot duration is observed, from (3.1) we get

$$\begin{aligned} p_{d_{slot}}^{(1)} &= \int_0^{\infty} (1 - F_1(\tau))^{2559} f_{Y_1(0)|(N_1=1)}(\tau) d\tau \\ &= \int_0^{\infty} \left(1 - e^{-\frac{\tau}{2}}\right)^{2559} \frac{e^{-\frac{\tau}{2(1+E_{s,PSCH}/I_0)}}}{2(1+E_{s,PSCH}/I_0)} d\tau. \end{aligned} \quad (3.2)$$

The integral can be expressed using integration by parts as

$$p_{d_{slot}}^{(1)} = \frac{2559!(1+E_{s,PSCH}/I_0)^{2559}}{\prod_{i=1}^{2559} (1+i(1+E_{s,PSCH}/I_0))}. \quad (3.3)$$

With the assumption that signals undergo independent Rayleigh fading in successive slots, we can

obtain  $p_d^{(1)}$  as below

$$p_d^{(1)} = 1 - p_e^{(1)} = 1 - \sum_{n=0}^{N_1} p(\text{error}|n \text{ slot correct})p(n \text{ slot correct}), \quad (3.4)$$

where  $p(n \text{ slot correct}) = \text{binopdf}(n, N_1, p_{d_{\text{slot}}}^{(1)})$  and  $\text{binopdf}(n, N_1, p_{d_{\text{slot}}}^{(1)})$  is the Binomial pdf with parameters  $N_1$  and  $p_{d_{\text{slot}}}^{(1)}$  evaluated at  $n$  defined as [18]

$$\text{binopdf}(n, N_1, p_{d_{\text{slot}}}^{(1)}) = \begin{cases} \binom{N_1}{n} (p_{d_{\text{slot}}}^{(1)})^n (1 - p_{d_{\text{slot}}}^{(1)})^{N_1-n} & n = 0, 1, 2, \dots, N_1 \\ 0 & \text{otherwise.} \end{cases} \quad (3.5)$$

It is clear that  $\Pr(\text{error}|0 \text{ slot correct}) = 1$ . Examination of simulation results revealed that for  $N_1 = 15$ ,  $\Pr(\text{error}|1 \text{ slot correct}) \approx 0.93$  and  $\Pr(\text{error}|n \text{ slot correct}) \approx 0, n = 2, 3, \dots, 15$ . Therefore, the probability of correctly selecting the slot boundary with the most frequent occurrence slot synchronization technique under independent Rayleigh fading is

$$p_d^{(1)} = 1 - \text{binopdf}(0, 15, p_{d_{\text{slot}}}^{(1)}) - 0.93 \times \text{binopdf}(1, 15, p_{d_{\text{slot}}}^{(1)}). \quad (3.6)$$

### 3.1.2 Block Rayleigh Fading Model

In this model, we assume that the fading is constant over  $N_1$  time slots, i.e.  $X_i = X$  for  $0 \leq i \leq N_1 - 1$ , where  $X \sim N_c(0, E_{s, PSCH}/I_0)$ , changing from block to block.

#### 3.1.2.1 Accumulation Slot Synchronization Technique

As in the independent Rayleigh fading case, we get

$$p_d^{(1)} = \int_0^{\infty} (1 - F_{N_1}(\tau))^{2559} f_{Y_1(0)}(\tau) d\tau, \quad (3.7)$$

where  $F_{N_1}(\tau)$  is given by (2.4) and  $f_{Y_1(0)}(\tau)$  is given by (2.8).

### 3.1.2.2 Most Frequent Occurrence Slot Synchronization Technique

Under block Rayleigh fading, for any given  $|X|^2 = x$ ,  $Y_1(0)$  is non-central  $\chi^2$  distributed with  $2N_1$  degrees of freedom. First, from (2.7), when  $N_1 = 1$

$$f_{Y_1(0)||X|^2=x}(\tau) = \frac{1}{2} e^{-\frac{(x+\tau)}{2}} I_0(\sqrt{\tau x}). \quad (3.8)$$

Please note that the notation,  $I_0$ , used for the  $0^{th}$  order modified Bessel function of the first kind is the same as the notation for the background noise plus MAI variance. Based on the context, it should be simple to determine which one is used.

Therefore, for a given value of  $x$ , the probability of correctly selecting the slot boundary after observing one slot duration is

$$p_{d_{slot}}^{(1)} = \int_0^{\infty} (1 - F_1(\tau))^{2559} f_{Y_1(0)||X|^2=x}(\tau) d\tau, \quad (3.9)$$

From (3.6), it follows that for any given value of  $x$ , the probability of correctly choosing the slot boundary after observing 15 slot durations is

$$p_{d||X|^2=x}^{(1)} = 1 - \text{binopdf}\left(0, 15, p_{d_{slot}||X|^2=x}^{(1)}\right) - 0.93 \times \text{binopdf}\left(1, 15, p_{d_{slot}||X|^2=x}^{(1)}\right). \quad (3.10)$$

Since  $|X|^2$  is  $\chi^2$  distributed with 2 degrees of freedom, the probability of detection for stage 1 when the most frequent occurrence slot synchronization technique is used under block Rayleigh fading is

$$p_d^{(1)} = \int_0^\infty p_{d||X|^2=x}^{(1)} \frac{e^{\frac{-x}{2E_{s,PSCH}/I_0}}}{2E_{s,PSCH}/I_0} dx. \quad (3.11)$$

### 3.1.3 Independent Ricean Fading Model

When there is a nonfading signal component present, such as a line-of-sight propagation path, the small-scale fading envelope distribution is Ricean [19]. To model independent Ricean fading, we assume that the signal undergoes independent Ricean fading in successive slots, i.e.  $\{X_i, i = 1, 2, \dots, N_1 - 1\}$  are i.i.d complex Gaussian r.v.'s, each with mean  $m$  and variance  $\sigma^2$ . Then  $((X_i + n_i^u) \sim N_c(m, \sigma^2 + 1))$  and  $Y_1(0)$  is non-central  $\chi^2$  distributed with  $2N_1$  degrees of freedom, and we get [16]

$$f_{Y_1(0)}(\tau) = \frac{1}{2(\sigma^2 + 1)} \left( \frac{\tau}{2N_1 m^2} \right)^{\frac{N_1 - 1}{2}} e^{\frac{(2N_1 m^2 + \tau)}{2(\sigma^2 + 1)}} I_{N_1 - 1} \left( \frac{\sqrt{2N_1 \tau m^2}}{\sigma^2 + 1} \right), \quad (3.12)$$

where

$$\sigma^2 + m^2 = E_{s,PSCH}/I_0, \quad (3.13)$$

to ensure that the total received energy to interference ratio for the P-SCH is  $E_{s, PSCH}/I_0$ .

### 3.1.3.1 Accumulation Slot Synchronization Technique

From (2.5), the probability of detection for stage 1 is

$$p_d^{(1)} = \int_0^{\infty} (1 - F_{N_1}(\tau))^{2559} f_{Y_1(0)}(\tau) d\tau, \quad (3.14)$$

where  $F_{N_1}(\tau)$  is given by (2.4), and  $f_{Y_1(0)}(\tau)$  is given by (3.12).

### 3.1.3.2 Most Frequent Occurrence Slot Synchronization Technique

First we consider the probability of detection when only one slot duration is observed, from (3.14) when  $N_1 = 1$  we get

$$p_{d_{slot}}^{(1)} = \int_0^{\infty} (1 - F_1(\tau))^{2559} f_{Y_1(0)|(N_1=1)}(\tau) d\tau. \quad (3.15)$$

where  $f_{Y_1(0)|(N_1=1)}(\tau)$  can be obtained from (3.12). With the assumption that signals undergo independent Ricean fading in successive slots,  $p_d^{(1)}$  is given by (3.6)

$$p_d^{(1)} = 1 - \text{binopdf}(0, 15, p_{d_{slot}}^{(1)}) - 0.93 \times \text{binopdf}(1, 15, p_{d_{slot}}^{(1)}). \quad (3.16)$$

### 3.1.4 Block Ricean Fading Model

In this model, we assume that the fading is constant over  $N_1$  time slots (one block), i.e.

$X_i = X$  for  $0 \leq i \leq N_1 - 1$ , where  $X$  is i.i.d Gaussian r.v. each with mean  $m$  and variance  $\sigma^2$

$(X \sim N_c(m, \sigma^2))$ , changing from block to block. Within a block, for a given value  $x$  of the r.v.

$|X|^2$ ,  $Y_1(0)$  is non-central  $\chi^2$  distributed with  $2N_1$  degrees of freedom and the conditional pdf

$f_{Y_1(0)|X|^2=x}(\tau)$  is given by [16]

$$f_{Y_1(0)|X|^2=x}(\tau) = \frac{1}{2} \left( \frac{\tau}{N_1 x} \right)^{\frac{N_1-1}{2}} e^{-\frac{(N_1 x + \tau)}{2}} I_{N_1-1}(\sqrt{N_1 \tau x}), \quad (3.17)$$

where  $I_{N_1-1}(x)$  is the  $(N_1 - 1)^{th}$  order modified Bessel function of the first kind. Since  $|X|^2$  is non-central  $\chi^2$  distributed with 2 degrees of freedom, the pdf of  $Y_1(0)$  for the block Ricean fading model can be written as

$$f_{Y_1(0)}(\tau) = \int_0^\infty f_{Y_1(0)|X|^2=x}(\tau) \frac{1}{2\sigma^2} e^{-\frac{(2m^2+x)}{2\sigma^2}} I_0\left(\frac{\sqrt{2xm^2}}{\sigma^2}\right) dx. \quad (3.18)$$

#### 3.1.4.1 Accumulation Slot Synchronization Technique

As shown in the independent Rayleigh fading case, we get from (2.5)

$$p_d^{(1)} = \int_0^\infty (1 - F_{N_1}(\tau))^{2559} f_{Y_1(0)}(\tau) d\tau, \quad (3.19)$$

where  $f_{Y_1(0)}(\tau)$  is given by (3.19).

#### 3.1.4.2 Most Frequent Occurrence Slot Synchronization Technique

In block Ricean fading, for any given  $|X|^2 = x$ ,  $Y_1(0)$  is non-central  $\chi^2$  distributed with



$2N_1$  degrees of freedom. First, from (3.17), when  $N_1 = 1$

$$f_{Y_1(0)||X|^2=x}(\tau) = \frac{1}{2} e^{-\frac{(x+\tau)}{2}} I_0(\sqrt{\tau x}). \quad (3.20)$$

Therefore, from (3.19) and (3.20) for a given value  $x$ , the probability of correctly selecting the slot boundary after observing one slot duration is

$$p_{d_{slot}||X|^2=x}^{(1)} = \int_0^{\infty} (1 - F_{N_1=1}(\tau))^{2559} f_{Y_1(0)||X|^2=x}(\tau) d\tau. \quad (3.21)$$

From (3.6), it follows that for a given value  $x$ , the probability of correctly choosing the slot boundary after observing 15 slot durations is

$$p_{d||X|^2=x}^{(1)} = 1 - \text{binopdf}\left(0, 15, p_{d_{slot}||X|^2=x}^{(1)}\right) - 0.93 \times \text{binopdf}\left(1, 15, p_{d_{slot}||X|^2=x}^{(1)}\right). \quad (3.22)$$

Since  $|X|^2$  is non-central  $\chi^2$  distributed with 2 degrees of freedom, the probability of detection for stage 1 when the most frequent occurrence slot synchronization technique is used under block Ricean fading is

$$p_d^{(1)} = \int_0^{\infty} p_{d||X|^2=x}^{(1)} \frac{1}{2\sigma^2} e^{-\frac{(2m^2+x)}{2\sigma^2}} I_0\left(\frac{\sqrt{2xm^2}}{\sigma^2}\right) dx. \quad (3.23)$$

### 3.2 Stage 2 Analysis

Given the slot boundary information, the input signal for every slot is correlated with the 16 possible SSCs to give an estimate of which one of the 16 SSCs was transmitted. After  $N_2$  slots,

the  $N_2$  decision variables are correlated against the 64 possible frame SYNC sequences and their 14 cyclic shifts. The Frame SYNC sequence with the cyclic shift that produces the maximum correlation value is chosen as the code group estimate.

When correlating the input signals with the 16 SSCs, the result r.v.  $Y_2(v)$  at the output of the correlator is defined as follows

$$Y_2(v) = \left| \sum_{j=0}^{255} y_j C_{SSC, v_j} \right|^2, \quad (3.24)$$

where  $y_i$  are the received slot aligned complex signals, sampled at chip intervals, with  $y_0$  being the first sample received when stage 2 begins;  $C_{SSC, v}$  is the  $v^{th}$  SSC. Without loss of generality, assuming that  $C_{SSC, 0}$  is the correct SSC, (3.24) implies

$$Y_2(v) \cong \begin{cases} |X + n_i^{(v)}|^2, v = 0 & \text{correct SSC hypothesis} \\ |n_i^{(v)}|^2, v \neq 0 & \text{incorrect SSC hypothesis,} \end{cases} \quad (3.25)$$

where  $0 \leq v \leq 15$  because there are 16 possible SSCs.

### 3.2.1 Independent Rayleigh Fading

In order to determine the probability of selecting the correct code group and the frame boundary, we first need to determine the probability of correctly detecting the SSC in every slot. The approach taken to calculate the probability of correct detection of the SSC is similar to that of the stage 1 probability of detection. Let  $p_{d_{SSC}}^{(2)}$  be the probability of correctly detecting the SSC in

stage 2, then

$$p_{d_{SSC}}^{(2)} = \int_0^{\infty} (1 - F_1(\tau))^{15} f_{Y_2(0)}(\tau) d\tau, \quad (3.26)$$

where  $1 - F_1(\tau)$  is the probability that  $Y_2(v) \leq \tau$ ,  $v \neq 0$  and  $f_{Y_2(0)}(\tau)$  is the pdf of  $Y_2(0)$  as given by (2.6). The term  $(1 - F_1(\tau))^{15}$  accounts for the fact that there are 15 non-zero values of  $v$ , i.e.  $v = 1, 2, \dots, 15$ . Substituting (2.6) into (3.26) yields

$$\begin{aligned} p_{d_{SSC}}^2 &= \int_0^{\infty} \left(1 - e^{-\frac{\tau}{2}}\right)^{15} \frac{e^{-\frac{\tau}{2(1+E_{s,SSCH}/I_0)}}}{2(1+E_{s,SSCH}/I_0)} d\tau \\ &= \frac{15!(1+E_{s,SSCH}/I_0)^{15}}{\prod_{i=1}^{15} (1+i(1+E_{s,SSCH}/I_0))}, \end{aligned} \quad (3.27)$$

where  $E_{s,SSCH}/I_0$  is the symbol energy to interference ratio on the S-SCH.

Let  $p_d^{(2)}$  be the probability of determining the code group and frame boundary when  $N_2 = 15$  slot durations are observed in stage 2. Examination of the simulation results revealed that when more than 6 slots within a frame are detected correctly,  $p_d^{(2)} \approx 1$ ; when 5 slots within a frame are detected correctly,  $p_d^{(2)} \approx 0.5$ ; when less than 4 slots are detected correctly,  $p_d^{(2)} \approx 0$ . Since we are assuming that successive slots undergo independent Rayleigh fading, we can write

$$p_d^{(2)} = 1 - (\text{binocdf}(4, 15, p_{d_{SSC}}^{(2)}) + 0.5 \text{binopdf}(5, 15, p_{d_{SSC}}^{(2)})), \quad (3.28)$$

where  $\text{binocdf}$  is the cdf of the binomial distribution.

### 3.2.2 Block Rayleigh Fading Model

For any given value  $x$  of the r.v.  $|X|^2$ , the probability of correctly detecting the SSC is

$$p_{d_{SSC}|X|^2=x}^{(2)} = \int_0^\infty (1 - F_1(\tau))^{15} f_{Y_2(0)|X|^2=x}(\tau) d\tau, \quad (3.29)$$

where  $f_{Y_2(0)|X|^2=x}$  is given by (3.8). Thus from (3.28), it follows that for any given  $x$ , the probability of correctly estimating the code group and frame boundary is

$$p_{d|X|^2=x}^{(2)} = 1 - \text{binopdf}\left(4, 15, p_{d_{SSC}|X|^2=x}^{(2)}\right) - 0.5 \times \text{binopdf}\left(5, 15, p_{d_{SSC}|X|^2=x}^{(2)}\right). \quad (3.30)$$

Since  $|X|^2$  is central  $\chi^2$  distributed with 2 degrees of freedom, the probability of detection for stage 2 under block Rayleigh fading is

$$p_d^{(2)} = \int_0^\infty p_{d|X|^2=x}^{(2)} \frac{e^{-x/2E_{s,SSCH}/I_0}}{2E_{s,SSCH}/I_0} dx. \quad (3.31)$$

### 3.2.3 Independent Ricean Fading Model

Here again, we can express the probability of SSC detection as

$$p_{d_{SSC}}^{(2)} = \int_0^\infty (1 - F_1(\tau))^{15} f_{Y_2(0)}(\tau) d\tau, \quad (3.32)$$

where  $f_{Y_2(0)}(\tau)$  is given by (3.12), so that (3.32) becomes

$$p_{d_{ssc}}^{(2)} = \int_0^\infty \left(1 - e^{-\frac{\tau}{2}}\right)^{15} \frac{1}{2\sigma^2} e^{-\frac{(2m^2 + \tau)}{2\sigma^2}} I_0\left(\frac{\sqrt{2\tau m^2}}{\sigma^2}\right) d\tau. \quad (3.33)$$

As in (3.28), the probability of correctly detecting the code group and the frame boundary is given by

$$p_d^{(2)} = 1 - (\text{binocdf}(4, 15, p_{d_{ssc}}^{(2)}) + 0.5 \text{binopdf}(5, 15, p_{d_{ssc}}^{(2)})). \quad (3.34)$$

### 3.2.4 Block Ricean Fading Model

For any given value  $x$  of the r.v.  $|X|^2$ , the probability of correctly detecting the SSC is

$$p_{d_{ssc}|X|^2=x}^{(2)} = \int_0^\infty (1 - F_1(\tau))^{15} f_{Y_2(0)|X|^2=x}(\tau) d\tau, \quad (3.35)$$

where  $f_{Y_2(0)|X|^2=x}$  is given by (3.8). As in (3.28), for any given value  $x$  of the r.v.  $|X|^2$ , the probability of correctly detecting the code group and frame boundary is

$$p_{d|X|^2=x}^{(2)} = 1 - \text{binopdf}\left(4, 15, p_{d_{ssc}|X|^2=x}^{(2)}\right) - 0.5 \times \text{binopdf}\left(5, 15, p_{d_{ssc}|X|^2=x}^{(2)}\right). \quad (3.36)$$

Since  $|X|^2$  is non-central  $\chi^2$  distributed with 2 degrees of freedom, the probability of detection for stage 2 under block Ricean fading is

$$p_d^{(2)} = \int_0^\infty p_{d||X|^2=x}^{(2)} \frac{1}{2\sigma^2} e^{-\frac{(2m^2+x)}{2\sigma^2}} I_0\left(\frac{\sqrt{2xm^2}}{\sigma^2}\right) dx. \quad (3.37)$$

### 3.3 Stage 3 Analysis

The probability of detection analysis of stage 3 for Rayleigh fading is reviewed in this section followed by the analysis for Ricean fading.

#### 3.3.1 Rayleigh Fading Model

The probability of correct detection in Rayleigh fading is given by (2.11) which is reproduced for convenience

$$\begin{aligned} p_d^{(3)} &= \int_0^\infty (1 - F_1(\tau))^7 f_{Y_3(0)}(\tau) d\tau = \int_0^\infty \left(1 - e^{-\frac{\tau}{2}}\right)^7 \frac{e^{-\frac{\tau}{2(1+E_{s,CPICH}/I_0)}}}{2(1+E_{s,CPICH}/I_0)} d\tau \\ &= \frac{7!(1+E_{s,CPICH}/I_0)^7}{\prod_{i=1}^7 (1+i(1+E_{s,CPICH}/I_0))}, \end{aligned} \quad (3.38)$$

where  $E_{s,CPICH}/I_0$  is the symbol energy to interference ratio for the CPICH used in stage 3 detection.

#### 3.3.2 Ricean Fading Model

The method for analyzing the probability of choosing the correct scrambling code for Ricean fading is very similar to that for Rayleigh fading. The main difference is that  $f_{Y_3(0)}(\tau)$  is now non-central  $\chi^2$  distributed with 2 degrees of freedom instead of central  $\chi^2$  distributed.

Substituting the non-central  $\chi^2$  pdf with 2 degrees of freedom for  $f_{Y_3(0)}(\tau)$  yields

$$p_d^{(3)} = \int_0^\infty \left(1 - e^{-\frac{\tau}{2}}\right)^7 \frac{1}{2\sigma^2} e^{-\frac{(2m^2 + \tau)}{2\sigma^2}} I_0\left(\frac{\sqrt{2\tau m^2}}{\sigma^2}\right) d\tau, \quad (3.39)$$

where

$$\sigma^2 + m^2 = E_{s, CPICH}/I_0. \quad (3.40)$$

### 3.4 Mean Synchronization Time

We consider a serial configuration for the synchronization process. Each of the three previously described stages of the synchronization procedure requires some time for completion. However, due to the fact that the whole process operates at a non-zero error probability, it is likely that before achieving synchronization, the MS may have to repeat this process a number of times. The time required until the MS acquires synchronization is defined as the synchronization time. If the MS manages to synchronize at the  $m^{th}$  attempt, the resulting synchronization time is

$$T(m) = m \cdot (T_1 + T_2 + T_3) + (m - 1) \cdot T_{pen}, \quad (3.41)$$

where  $T_1, T_2, T_3$  is the duration of the first, second and third stage respectively, and  $T_{pen}$  is the penalty time. The sum  $T_1 + T_2 + T_3$ , will be referred to as the nominal synchronization time.

When the MS fails to synchronize at the end of stage 3, the synchronization procedure does not restart immediately. The penalty time,  $T_{pen}$ , accounts for the time spent by the MS to read the Broadcast channel (BCH) information, realize that an error has occurred, and finally

re-initiate the synchronization procedure [14].

### 3.4.1 Independent fading

Under the independent fading assumption, the three stages operate independently of each other. Assuming that the probability of success of the  $i^{th}$  stage is  $p_d^{(i)}$ , then the overall probability of cell search success of the synchronization procedure is

$$p = \prod_{i=1}^3 p_d^{(i)}. \quad (3.42)$$

The MS continuously tries to achieve synchronization with a probability of success given by (3.42). Thus, the number of attempts for achieving synchronization is geometrically distributed and the probability of achieving synchronization at the  $m^{th}$  attempt is given by

$$p(m) = (1 - p)^{m-1} p. \quad (3.43)$$

The mean synchronization time can be computed by

$$\begin{aligned} E[T] &= \sum_{m=1}^{\infty} (m(T_1 + T_2 + T_3) + (m-1)T_{pen})(1-p)^{m-1} p \\ &= (T_1 + T_2 + T_3)p \sum_{m=1}^{\infty} m(1-p)^{m-1} + T_{pen}p \sum_{m=1}^{\infty} (m-1)(1-p)^{m-1}. \end{aligned} \quad (3.44)$$

Using the fact that



$$\begin{aligned}
\sum_{m=1}^{\infty} (1-p)^{m-1} &= \frac{1}{p} \\
\sum_{m=1}^{\infty} m(1-p)^{m-1} &= \frac{1}{p^2} \\
\sum_{m=1}^{\infty} (m-1)(1-p)^{m-1} &= \frac{1-p}{p^2},
\end{aligned} \tag{3.45}$$

the average cell search time can be written as

$$E[T] = (T_1 + T_2 + T_3) \frac{1}{p} + T_{pen} \frac{(1-p)}{p}. \tag{3.46}$$

### 3.4.2 Block Fading

Under the block fading assumption, the 3 stages are no longer independent of each other. However, given a certain energy to interference ratio  $|X|^2 = x$ , the three stages undergo independent fading. Then the overall probability of cell search success becomes

$$p = \int_0^{\infty} p_{d||X|^2=x}^{(1)} p_{d||X|^2=x}^{(2)} p_{d||X|^2=x}^{(3)} f_{|X|^2}(x) dx, \tag{3.47}$$

where  $p_{d||X|^2=x}^{(i)}$  is the probability of detection for stage  $i$  given  $x$ , and  $f_x$  is the pdf of  $x$ .

When the accumulation method is used in stage 1, from (2.5) we can write  $p_{d||X|^2=x}^{(1)}$  as

$$p_{d||X|^2=x}^{(1)} = \int_0^{\infty} (1 - F_{N_1}(\tau))^{2559} f_{Y_1(0)||X|^2=x}(\tau) d\tau, \tag{3.48}$$

where  $f_{Y_1(0)||X|^2=x}(\tau)$  is given by (2.7).

When the most frequent occurrence method is used in stage 1,  $p_{d||X|^2=x}^{(1)}$  is given by (3.10).

For stage 2,  $p_{d||X|^2=x}^{(2)}$  is given by (3.30). For stage 3, from (2.11)  $p_{d||X|^2=x}^{(3)}$  can be expressed as

$$p_{d||X|^2=x}^{(3)} = \int_0^{\infty} (1 - F_{N_3=1}(\tau))^7 f_{Y_3(0)||X|^2=x}(\tau) d\tau, \quad (3.49)$$

where  $f_{Y_3(0)||X|^2=x}(\tau) = \frac{1}{2} e^{-\frac{(3.16x + \tau)}{2}} I_0(\sqrt{3.16x\tau})$ . Note that the factor 3.16 is introduced to (3.8) because the  $E_s/I_0$  for the CPICH is 5 dB higher than that of the P-SCH and S-SCH.

We know that under Rayleigh fading,  $|X|^2$  is central  $\chi^2$  distributed with 2 degrees of freedom, thus  $f_{|X|^2}(x)$  is

$$f_{|X|^2}(x) = \frac{e^{-\frac{x}{2E_{s,PSCH}/I_0}}}{2E_{s,PSCH}/I_0}. \quad (3.50)$$

We also know that under Ricean fading,  $|X|^2$  is non-central  $\chi^2$  distributed with 2 degrees of freedom, thus  $f_{|X|^2}(x)$  is

$$f_{|X|^2}(x) = \frac{1}{2\sigma^2} e^{-\frac{(2m^2+x)}{2\sigma^2}} I_0\left(\frac{\sqrt{2xm^2}}{\sigma^2}\right), \quad (3.51)$$

where  $\sigma^2 + m^2 = E_{s,PSCH}/I_0$ .

## Chapter 4 Results

In this chapter, numerical results calculated using the analytic expressions obtained in the previous chapter are presented. Computer simulation results are also presented to validate the analytic results.

### 4.1 The SPW™ Simulation Model

In this section, the system level parameters of the cell search model are first introduced followed by descriptions of the main blocks used in the fast cell search simulation model.

#### 4.1.1 System Level Parameters

The parameters in the system model of the cell search algorithm are shown in Table 4.1.

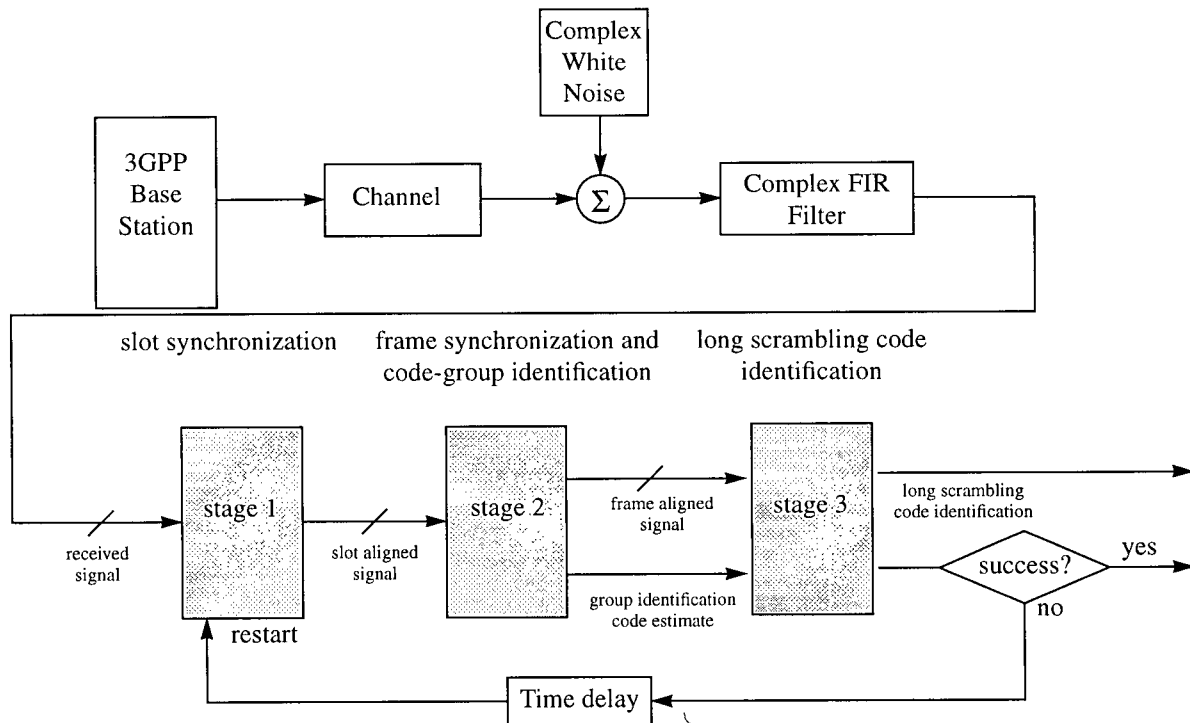
Name	Description	Default Value
chiprate	The fundamental chip rate for the model. This parameter is not intended to be changed.	3.86e6 chips/s
rxfile	An ASCII file with the coefficients for an SRRC filter with a roll-off factor of 0.22.	rcfilt1_16taps
numSlots	The number of slots used in deriving the estimate for the slot timing in stage 1.	15
codeMap	The file which contains the mapping for the code groups and is used for Frame SYNC detection.	gic_v320
bts_pwr	The total power transmitted from the base station. The power is normalized to 1 watt.	1 watt
cpichPower	The CPICH power in dB relative to the bts_pwr.	-10 dB
pccpchPower	The P-CCPCH power in dB relative to the bts_pwr.	-12 dB
pschPower	The P-SCH power in dB relative to the bts_pwr.	-15 dB
sschPower	The S-SCH power in dB relative to the bts_pwr.	-15 dB
pichPower	The PICH power in dB relative to the bts_pwr.	-10 dB
Ioc_dB	The total interference power in dBm at the receiver. The interference is modeled as AWGN. Hence this value sets the variance of the COMPLEX WHITE NOISE block in the system model.	-60 dBm

Name	Description	Default Value
IortoIoc	The total received power relative to the interference power in dB. This parameter is used in the channel model to set the power in every path to ensure the appropriate total power at the receiver input.	-8 dB
cfreq	The carrier frequency for the system. This parameter only affects the channel characteristics.	2.1125e9 Hz
chan_model	This parameter selects the Channel Model to be used throughout the simulation.	static
pwr_rice	This parameter represents the fraction of the total transmitted power in the line-of-sight path.	0.5
speed	The vehicle speed in km/h	3 km/h

Table 4.1 System level parameters for the SPW<sup>TM</sup> fast cell search model

### 4.1.2 The Description of SPW<sup>TM</sup> System Model

In this section, the SPW<sup>TM</sup> system model is introduced. As shown in Figure 4.1, the model consisting of the following blocks are described in the following sections.

Figure 4.1 The SPW<sup>TM</sup> fast cell search system model

### 4.1.2.1 The 3GPP Base Station

The 3GPP base station block generates all of the common base station channels as well as one orthogonal channel noise simulator (OCNS). The block can be used in conjunction with any dedicated channel configuration to produce the complete signal transmitted from the base station.

The channels include:

- The common pilot channel (CPICH)
- The primary common control physical channel (P-CCPCH)
- The paging indicator channel (PICH)
- The primary synchronization channel (P-SCH)
- The secondary synchronization channel (S-SCH)
- The orthogonal channel noise simulator (OCNS)

The power levels for these channels are set according to the system level parameters used by the block. The OCNS power is calculated to make the total power equal to the power of the base station. In other words, the sum of the powers of all channels should be less than the system level parameter *bts\_pwr*. The PICH and P-CCPCH and OCNS are not used by the receiver in the cell search procedure and are provided only to set the proper level of interference.

The P-SCH and S-SCH are not scrambled. The other channels are summed and scrambled with the primary scrambling sequence. Before transmission, all signals pass through a shaping filter to limit their spectra. This is done using a Square Root Raised Cosine (SRRC) filter with a roll-off factor of 0.22.

#### 4.1.2.2 Channel

It is assumed that the channel undergoes single path slow fading, whose amplitude is Rayleigh or Ricean distributed. In the Ricean fading case, 50% of the total power is allocated to the line of sight path and the other 50% is allocated to the diffused path, i.e. Ricean factor of 0 dB.

#### 4.1.2.3 Complex White Noise

This block simulates the effect of interference in the system including inter-cell interference and thermal noise. The interference and noise are modeled as additive complex white Gaussian r.v.'s. The level of inter-cell interference is denoted by  $I_{oc}$  in dBm. To set the appropriate value of noise variance in the complex white noise block,  $I_{oc}$  is converted to linear power in Watts. The relationship between  $I_{oc}$  and the noise variance  $\sigma_{noise}^2$  is

$$\sigma_{noise}^2 = 10^{\frac{I_{oc} - 30}{10}}. \quad (4.1)$$

#### 4.1.2.4 Complex FIR Filter

The received signal is passed through a SRRC filter with identical parameters as that in the transmitter. This block is the frequency domain Finite Impulse Response (FIR) implementation of the SRRC filter and hence uses the same impulse response signal file as the transmit side.

#### 4.1.2.5 Slot Synchronization

This block is the first stage of the algorithm as discussed in Section 2.3.1. The block searches for the P-SCH sent by the base station. The P-SCH is sent during the first 1/10th of each slot. This block correlates the received signal with the 256 chips long PSC and looks for peaks to determine when the slot starts. It then aligns the input signal to be on a slot boundary.

#### 4.1.2.6 Code Group Identification and Frame Synchronization

This block is the second stage of the algorithm as discussed in Section 2.3.2. The block takes the slot aligned signal from the output of stage 1 and decodes the S-SCH to estimate the frame start and the primary scrambling sequence code group. The block outputs these estimates along with the received signal aligned to a frame boundary.

#### 4.1.2.7 Long Scrambling Code Identification

This block is the third stage of the algorithm as discussed in Section 2.3.3. The block takes the received signal aligned to a frame boundary and the primary scrambling sequence code group estimate and estimates the code number in the code group. The block outputs the estimated code number and the scrambling sequence associated with the code group and code number pair. The block correlates the received signal with all 8 possible primary scrambling sequences in the code group. At the end of each slot the correlator is dumped and the scrambling sequence with the greatest correlation is selected as the estimate. The block uses the fact that the CPICH is simply a constant multiplied by the primary scrambling sequence and so this channel will correlate well with the proper scrambling sequence generated by this block.

In our simulation, it is assumed that there are no sampling and frequency errors. A resolution of one chip is assumed for stage 1. In practice non-idealities in these functions will cause some degradation which are ignored in the simulation.

The SCH power is assumed to be equally divided between the P-SCH and S-SCH, and the CCPCH power is assumed to be equal to the SCH power. Two vehicle speeds of 3 km/h and 120 km/h for a carrier frequency of 2.1125 GHz are used in the simulation. This corresponds to Doppler frequencies of about 6 Hz and 235 Hz respectively. The simulation results for 3 km/h



agrees well with the analytical results of block Rayleigh fading case which assumes that the fading is constant over  $N_1 = 15$  slots. However, a Doppler frequency of 235 Hz does not closely match the independent Rayleigh fading assumption which results in some discrepancies between the simulation and analysis results.

## 4.2 Stage 1 Results

In this section, both theoretical and simulation results for slot synchronization probability are presented. First the results for Rayleigh fading are presented followed by those for Ricean fading.

### 4.2.1 Rayleigh Fading Model

In Figure 4.2, the theoretical slot synchronization probability is shown for  $N_1 = 15$  using the accumulation and most frequent occurrence techniques assuming independent Rayleigh fading. In the same graph, simulation results with a vehicular speed of 120 km/h are also shown. It can be seen that the accumulation technique outperforms the most frequent occurrence technique. For  $p_d^{(1)} = 0.5$ , there is about 3.5 dB gain when the accumulation technique is used compared to the most frequent occurrence technique.

The reason of the discrepancy between the theoretical and simulation results in Figure 4.2 is that the independent Rayleigh fading assumption is not closely satisfied. This reason explains the discrepancy between theoretical results assuming block fading and simulation results at a vehicular speed of 120 km/h in later sections as well.

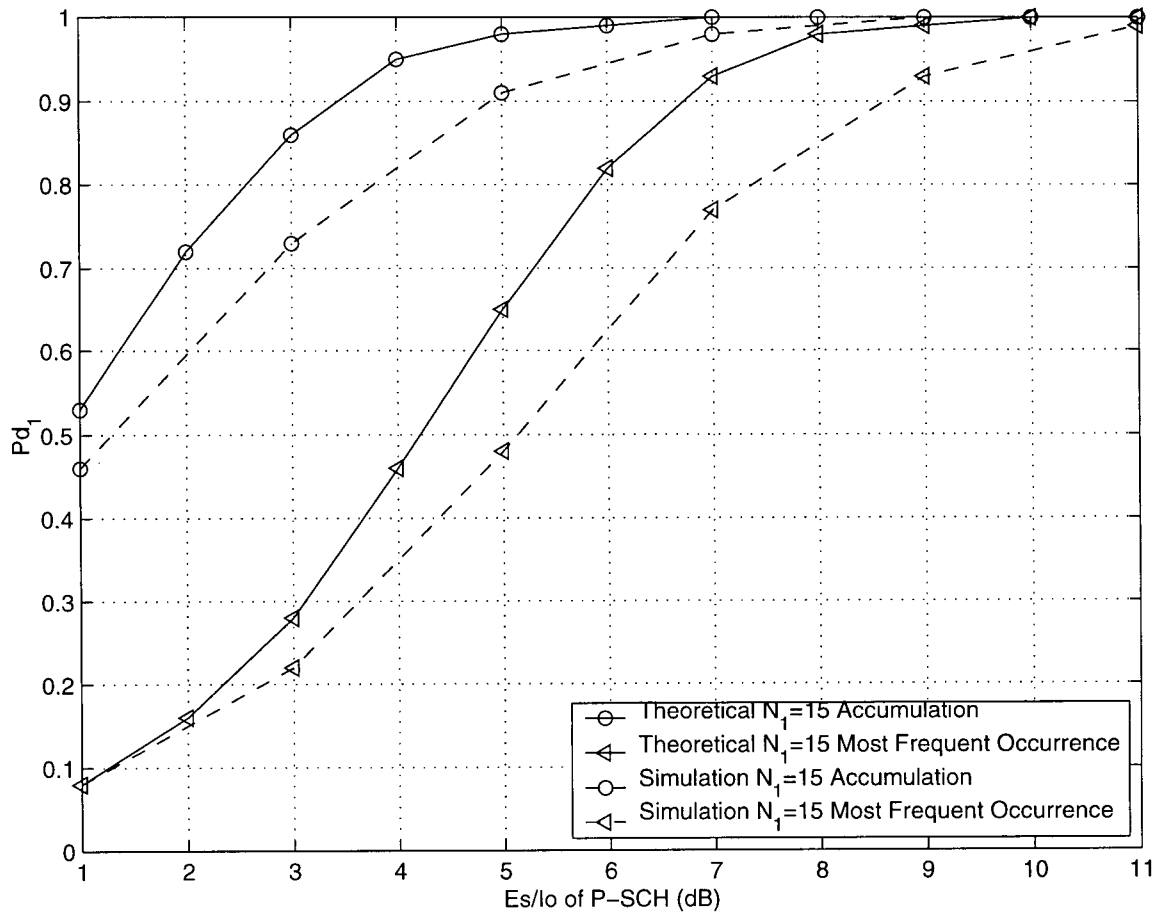


Figure 4.2 Stage 1 performance under independent Rayleigh fading channel

In Figure 4.3, the theoretical slot synchronization probability assuming block Rayleigh fading is shown for  $N_1 = 15$  using the accumulation and most frequent occurrence techniques. Also shown are simulation results with a vehicular speed of 3 km/h. In the present case, the accumulation technique outperforms the most frequent occurrence technique. For  $p_d^{(1)} = 0.5$ , there is about 4.5 dB gain when the accumulation technique is used compared to the most frequent occurrence technique. There is good agreement between the analytical and simulation results.

Comparing Figures 4.2 and 4.3, it can be seen that when the channel condition is good  $E_{s, PSCH} > 1$  dB, the detection probability for stage 1 is higher when vehicle speed is higher. However, with higher vehicle speeds, the detection probability degrades more rapidly when the channel condition deteriorates. An intuitive explanation for this observation is as follows: First, assuming that there is a threshold  $\theta$ . If the average  $E_{s, PSCH}/I_0$  for the 15 slots durations used in stage 1 detection is above  $\theta$ , the probability of correct detection for stage 1 is 100% and below which, the probability of correct detection is 0%. Considering that at high vehicular speeds, e.g. 120 km/h, 15 slot durations occupy approximately 5 fades and at low vehicular speeds, e.g. 3 km/h, 15 slot durations occupy only 1/10th of a fade, thus, when channel conditions are poor (assume that  $E_{s, PSCH}/I_0$  is above  $\theta$  for 5% of the time), the probability that the average  $E_{s, PSCH}/I_0$  is below  $\theta$  is then 100% for high vehicle speeds, e.g. 120 km/h. However, for low vehicular speeds, e.g. 3 km/h, the probability that the average  $E_{s, PSCH}/I_0$  is below  $\theta$  is less than 100%. On the other hand, when channel conditions are good (assume that  $E_{s, PSCH}/I_0$  is above  $\theta$  for 95% of the time), The probability that the average  $E_{s, PSCH}/I_0$  is above  $\theta$  is then 100% for high vehicle speeds, e.g. 120 km/h. However, for low vehicular speeds, e.g. 3 km/h, the probability that the average  $E_{s, PSCH}/I_0$  is above  $\theta$  is less than 100%.

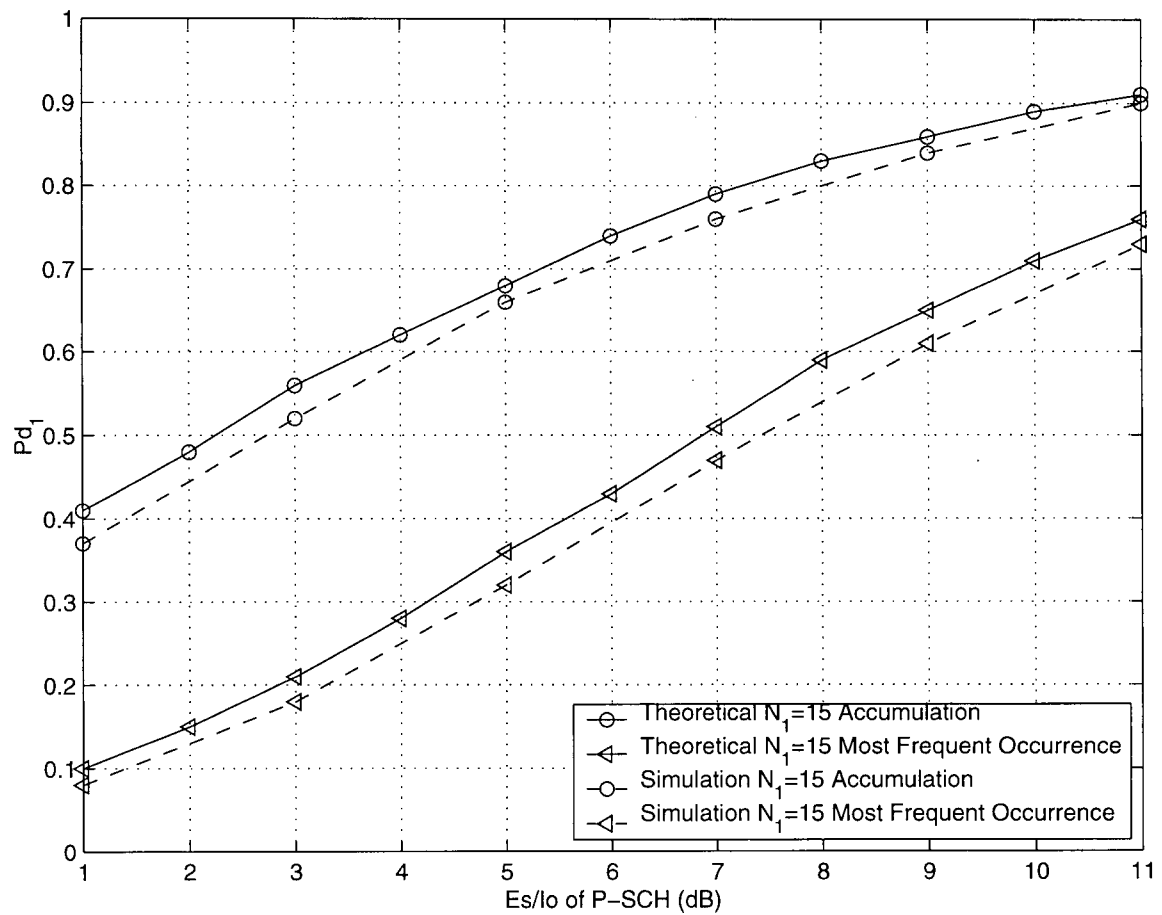


Figure 4.3 Stage 1 performance under block Rayleigh fading channel

### 4.2.2 Ricean Fading Model

In Figure 4.4, the theoretical slot synchronization probability is shown for  $N_1 = 15$  using the accumulation and most frequent occurrence techniques assuming independent Ricean fading. In the same graph, simulation results with a vehicular speed of 120 km/h are also shown. It can be seen that the accumulation technique outperforms the most frequent occurrence technique. For  $p_d^{(1)} = 0.5$ , there is about 4 dB gain when the accumulation technique is used compared to the most frequent occurrence technique.

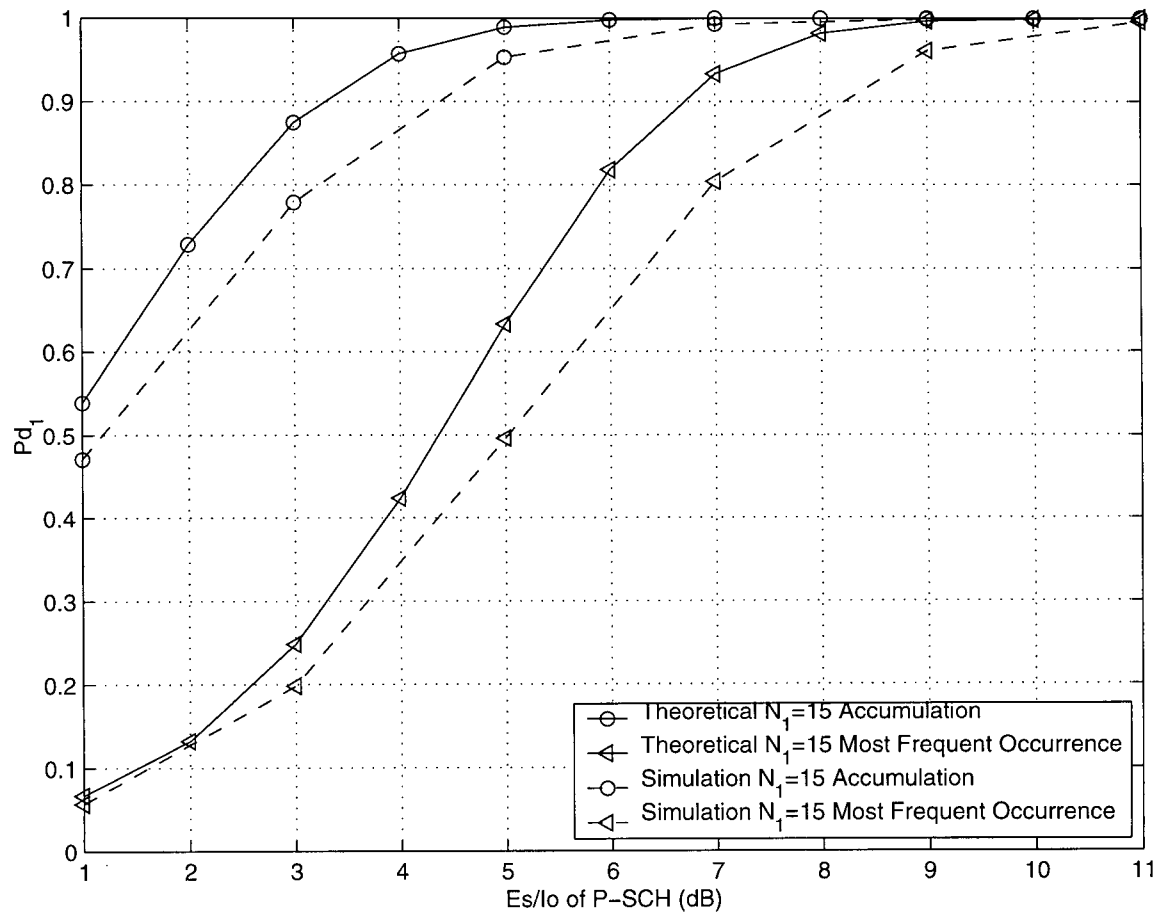


Figure 4.4 Stage 1 performance under independent Ricean fading channel

In Figure 4.5, the theoretical slot synchronization probability assuming block Ricean fading is shown for  $N_1 = 15$  using the accumulation and most frequent occurrence techniques. Also shown are simulation results with a vehicle speed of 3 km/h. The accumulation technique outperforms the most frequent occurrence technique. For  $p_d^{(1)} = 0.5$ , there is about 5 dB gain when the accumulation technique is used compared to the most frequent occurrence technique. There is also good agreement between the analytical and simulation results.

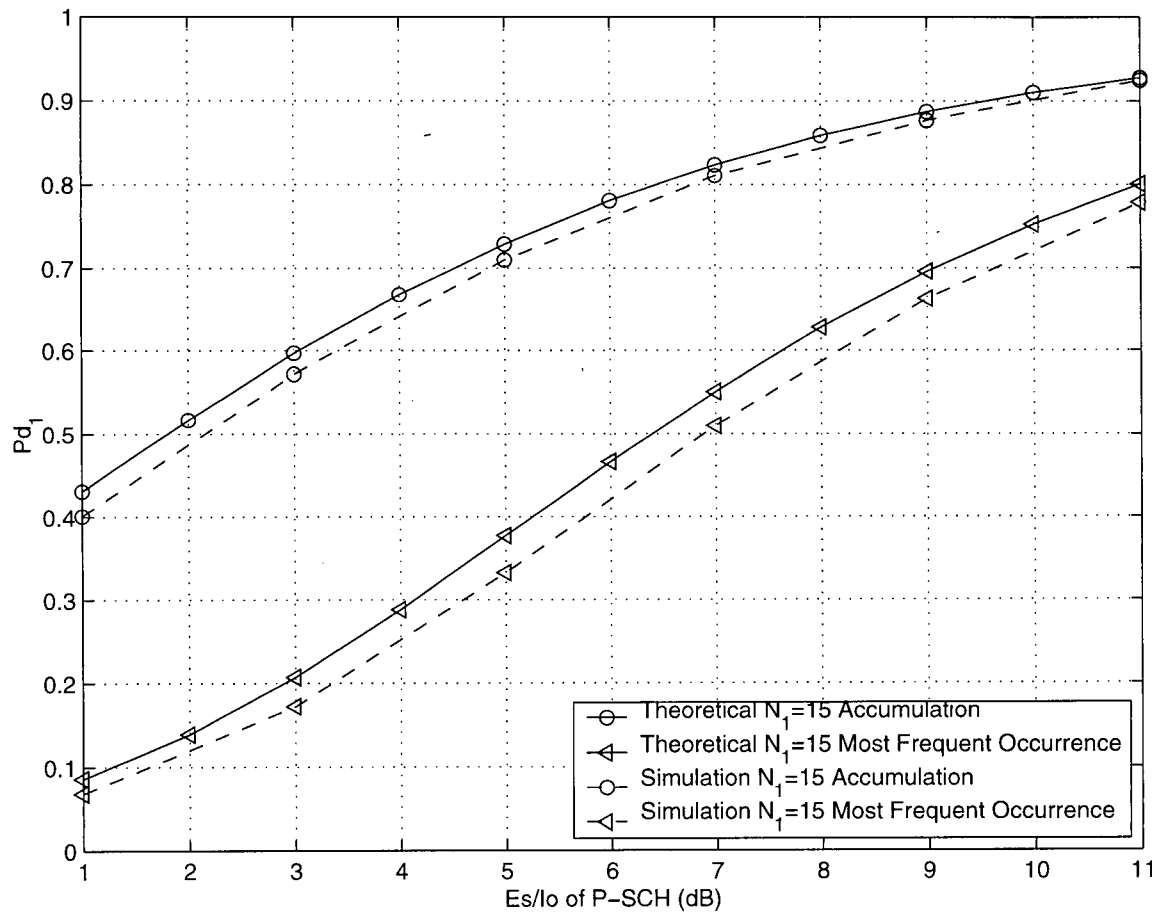


Figure 4.5 Stage 1 performance under block Ricean fading channel

Comparing Figures 4.4 and 4.5, we can see that when the channel condition is good,  $E_{s,PSCH} > 1$  dB, the detection probability for stage 1 is higher with faster vehicular speeds. However, with faster vehicle speed, the detection probability degrades more rapidly when the channel condition deteriorates.

A comparison of the Rayleigh and Ricean fading channel results in Figures 4.2 to 4.4 shows that the results for Ricean fading are slightly better, by about 0.5 dB.

### 4.3 Stage 2 Results

In this section, both theoretical and simulation results of stage 2 detection probability are presented. The results under Rayleigh fading are examined first followed by the results under Ricean fading channel.

#### 4.3.1 Rayleigh Fading Model

In Figure 4.6, the analytical and simulation results of SSC detection probability under Rayleigh fading are shown. It can be seen that there is good agreement between the analytical and simulation results.

The analytical and simulation results for stage 2 probability of detection are also presented in Figure 4.6. It can be seen that when  $E_{s_{SSCH}}/I_0 > 2$  dB the probability of detection for stage 2 at a vehicular speed of 120 km/h is higher than that of 3 km/h, but when  $E_{s_{SSCH}}/I_0$  continues to decrease, the probability of detection for a vehicular speed of 120 km/h degrades more rapidly.

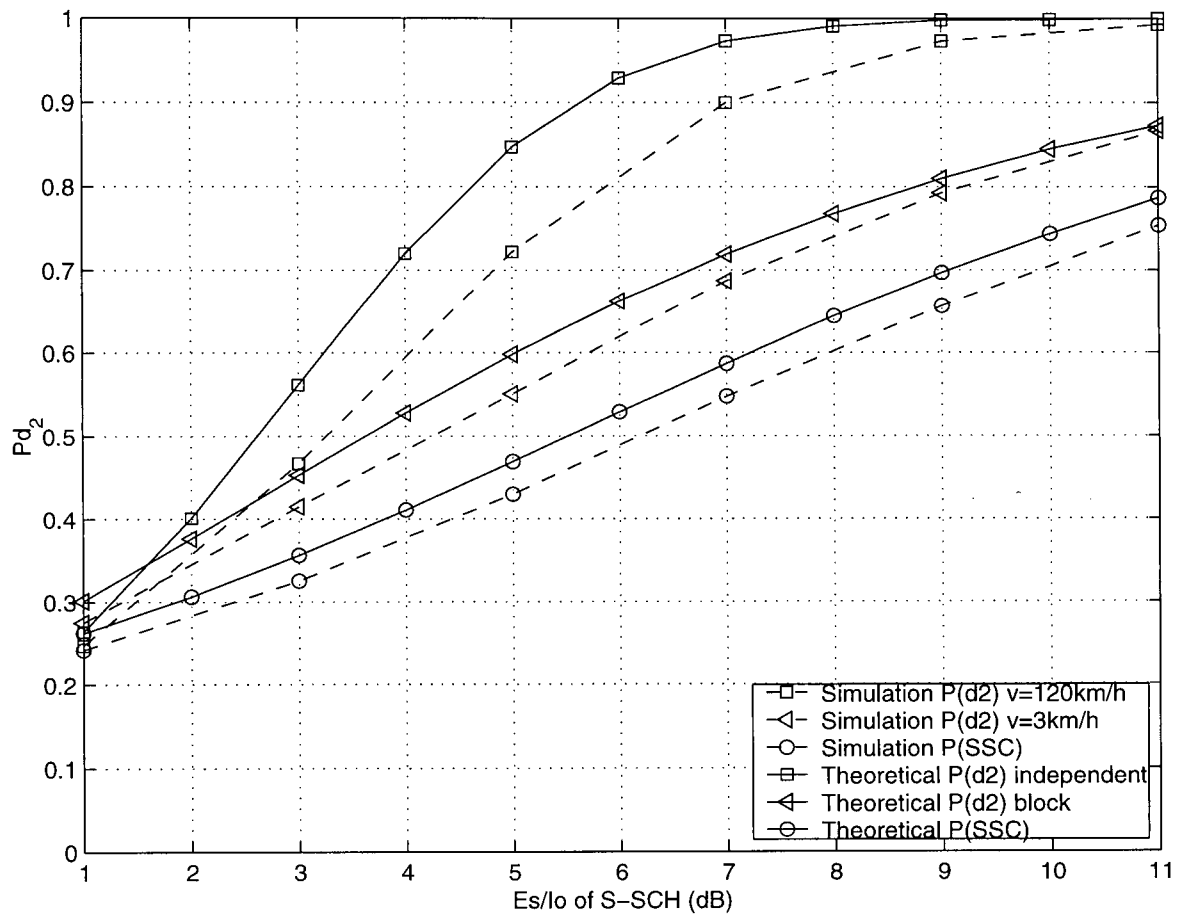


Figure 4.6 Stage 2 performance under Rayleigh fading channel

### 4.3.2 Ricean Fading Model

In Figure 4.7, the theoretical and simulation results of SSC detection probability are shown. Also shown are the theoretical and simulation results for stage 2 probability of detection. It can be seen that the results for Ricean fading are slightly better than those for Rayleigh fading.



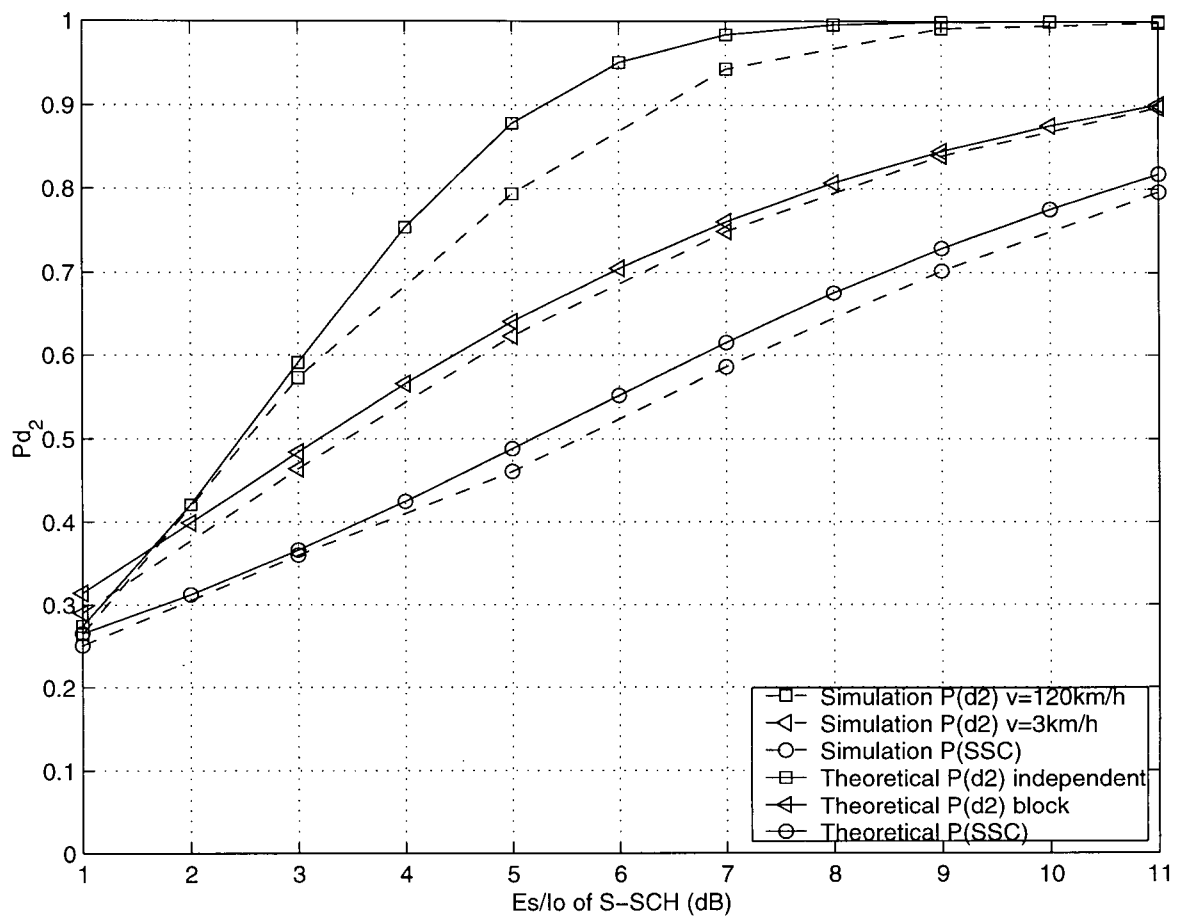


Figure 4.7 Stage 2 performance under Ricean fading channel

## 4.4 Stage 3 Results

In this section, the results of both the theoretical and simulation for stage 3 are presented. The results for Rayleigh fading are presented first followed by the results for Ricean fading.

### 4.4.1 Rayleigh Fading Model

As Figure 4.8 shows, the theoretical results are more optimistic, but the difference between the analytical and simulation results is quite small. As expected, the detection probability increases with  $E_s/I_0$ .

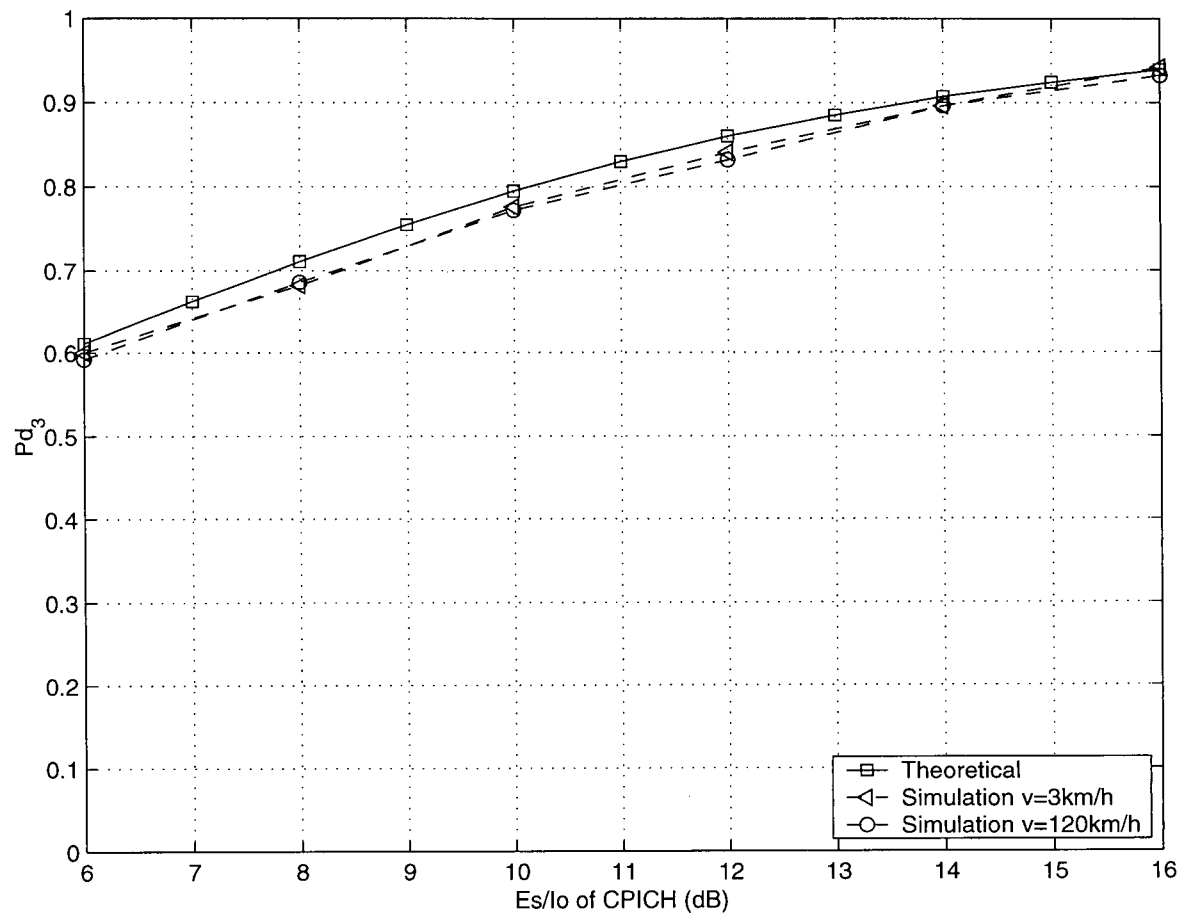


Figure 4.8 Stage 3 performance under Rayleigh fading channel

#### 4.4.2 Ricean Fading Model

As Figure 4.9 shows, there is good agreement between the analytical and simulation results for stage 3 probability of detection.

A comparison of the Rayleigh and Ricean fading channel results in Figures 4.8 and 4.9 shows that the results for Ricean fading are slightly better, by about 1 dB.

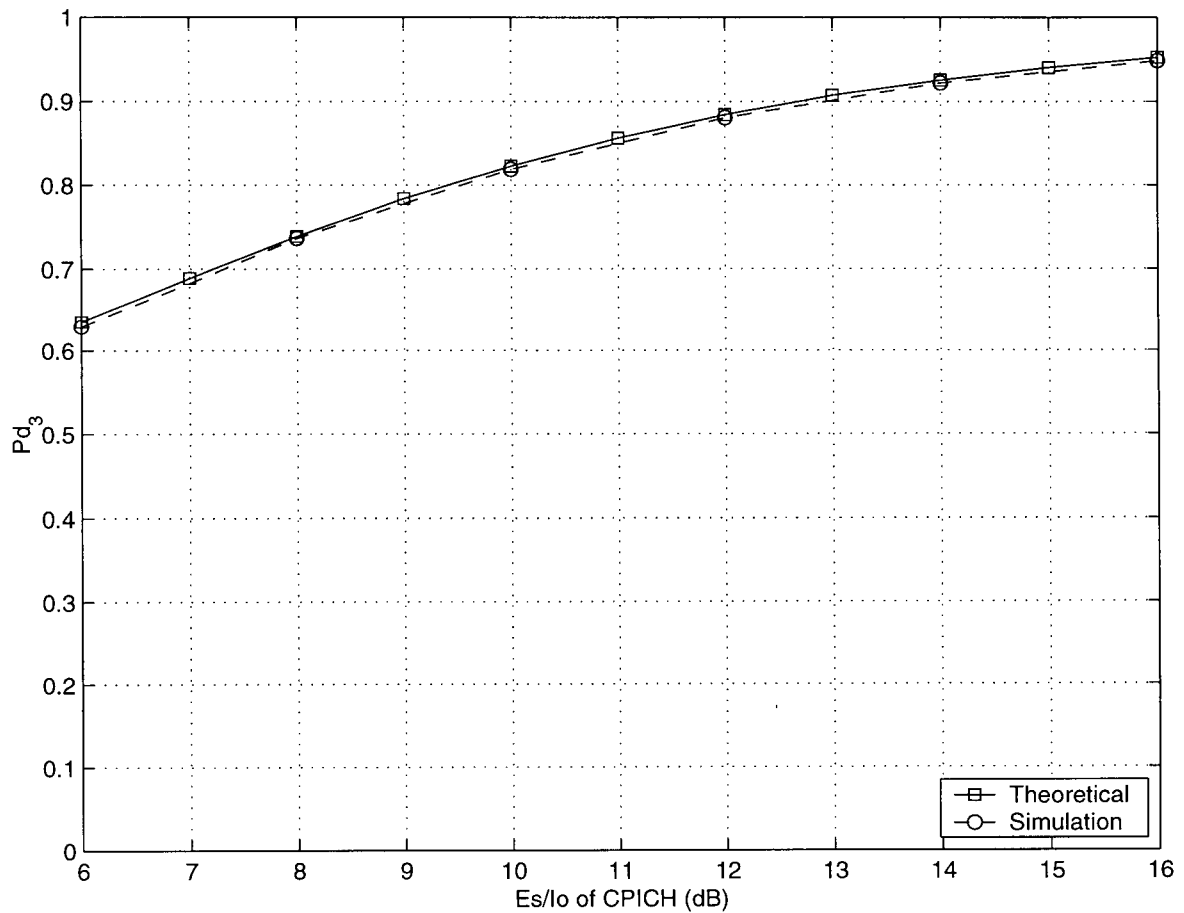


Figure 4.9 Stage 3 performance under Ricean fading channel

## 4.5 Mean Cell Search Time

In this section, both the theoretical and simulation results for the mean cell search time of the fast cell search algorithm are presented vs. the  $E_s/I_0$  of the SCH. First the results for Rayleigh fading are given followed by those for Ricean fading.

### 4.5.1 Rayleigh Fading Channel

In Figure 4.10, the theoretical results for the overall mean cell search time are presented assuming independent Rayleigh fading. Also shown are simulation results at a vehicular speed of

120 km/h. It can be seen that the mean cell search time increases rapidly when  $E_s/I_0$  is below about 7 dB. The mean cell search time is less for the accumulation method than the most frequent occurrence method and it increases as  $E_s/I_0$  is reduced. For the mean cell search time of 100 ms, the cell search algorithm using the accumulation technique has about 1.5 dB gain over the most frequent occurrence method and it increases as  $E_s/I_0$  is reduced. For the mean cell search time of 100 ms, the cell search algorithm using the accumulation technique has about 1.5 dB gain over the most frequent occurrence scheme. The reason for the difference between the analytical and simulation results Figure 4.10 is that the independent Rayleigh fading assumption is not closely satisfied.

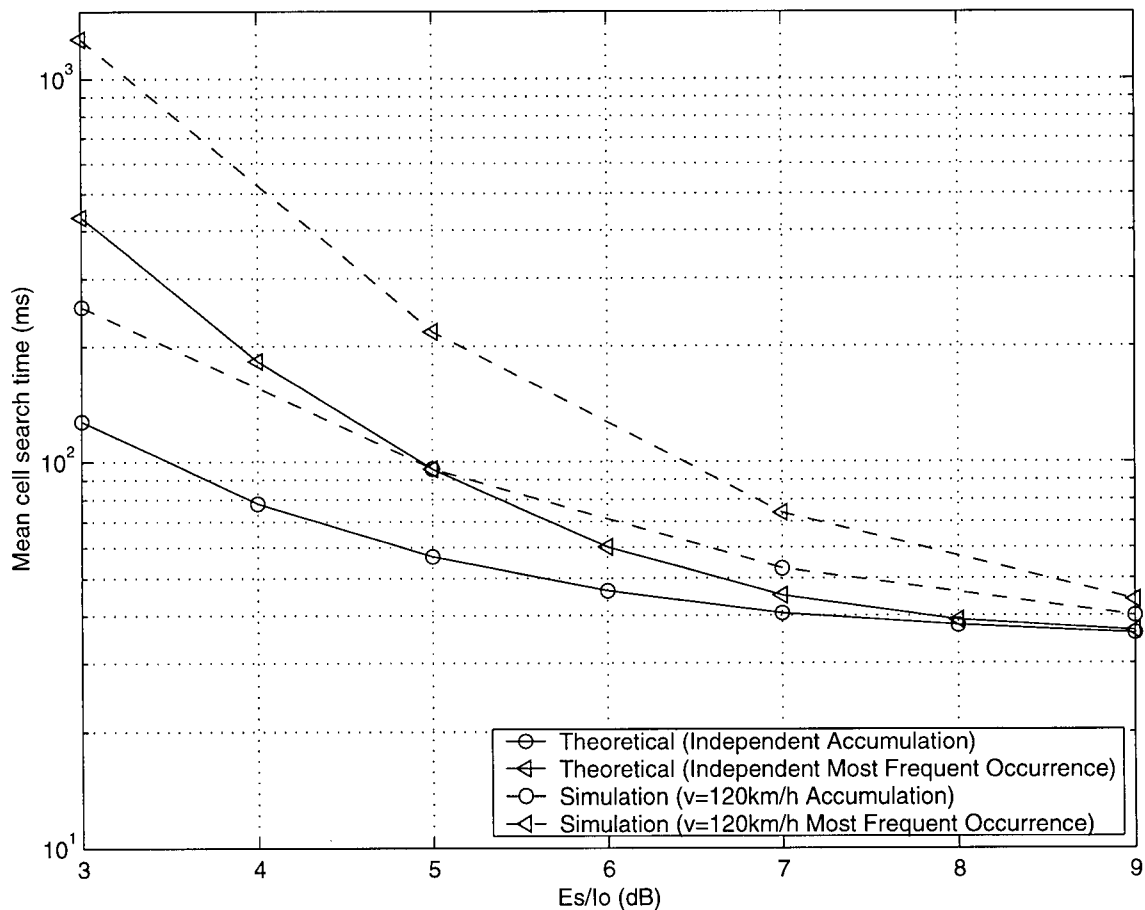


Figure 4.10 Mean cell search time under independent Rayleigh fading channel

In Figure 4.11, the theoretical results for the overall mean cell search time are presented

assuming block Rayleigh fading. Also shown are simulation results at a vehicular speed of 3 km/h. It can be seen that for the mean cell search time of 100 ms, the cell search algorithm using the accumulation technique has about 2.5 dB gain over the most frequent occurrence scheme. There is also a better agreement between the analytical and simulation results compared to results shown in Figure 4.10.

Comparing Figure 4.10 and Figure 4.11, it can be seen that the mean cell search time is less under independent fading when  $E_s/I_0$  is high, but increases more rapidly when  $E_s/I_0$  drops below 5 dB.

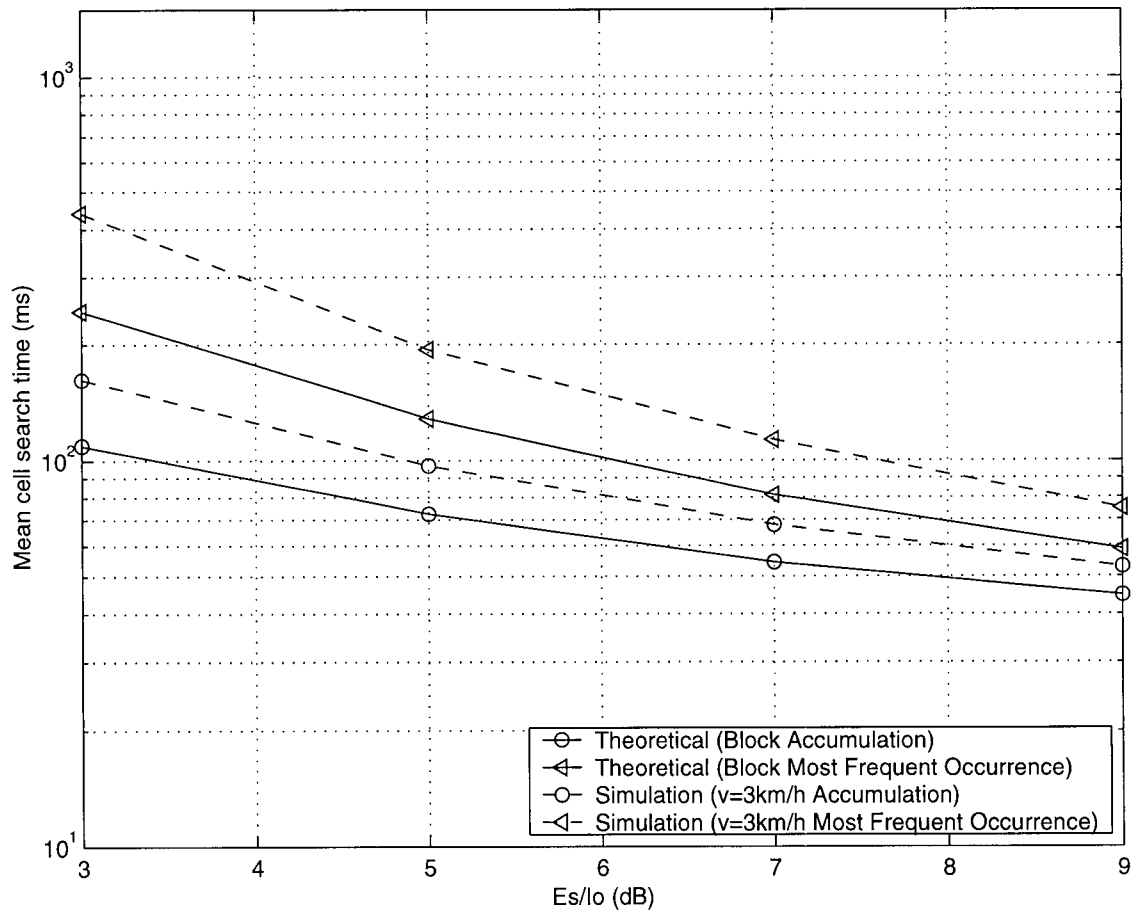


Figure 4.11 Mean cell search time under block Rayleigh channel

### 4.5.2 Ricean Fading Channel

In Figure 4.12, the theoretical results for the overall mean cell search time are presented assuming block Ricean fading. Also shown are simulation results at a vehicular speed of 120 km/h. It can be seen that for the mean cell search time of 100 ms, the cell search algorithm using the accumulation technique has about 1.5 dB gain over the most frequent occurrence scheme.

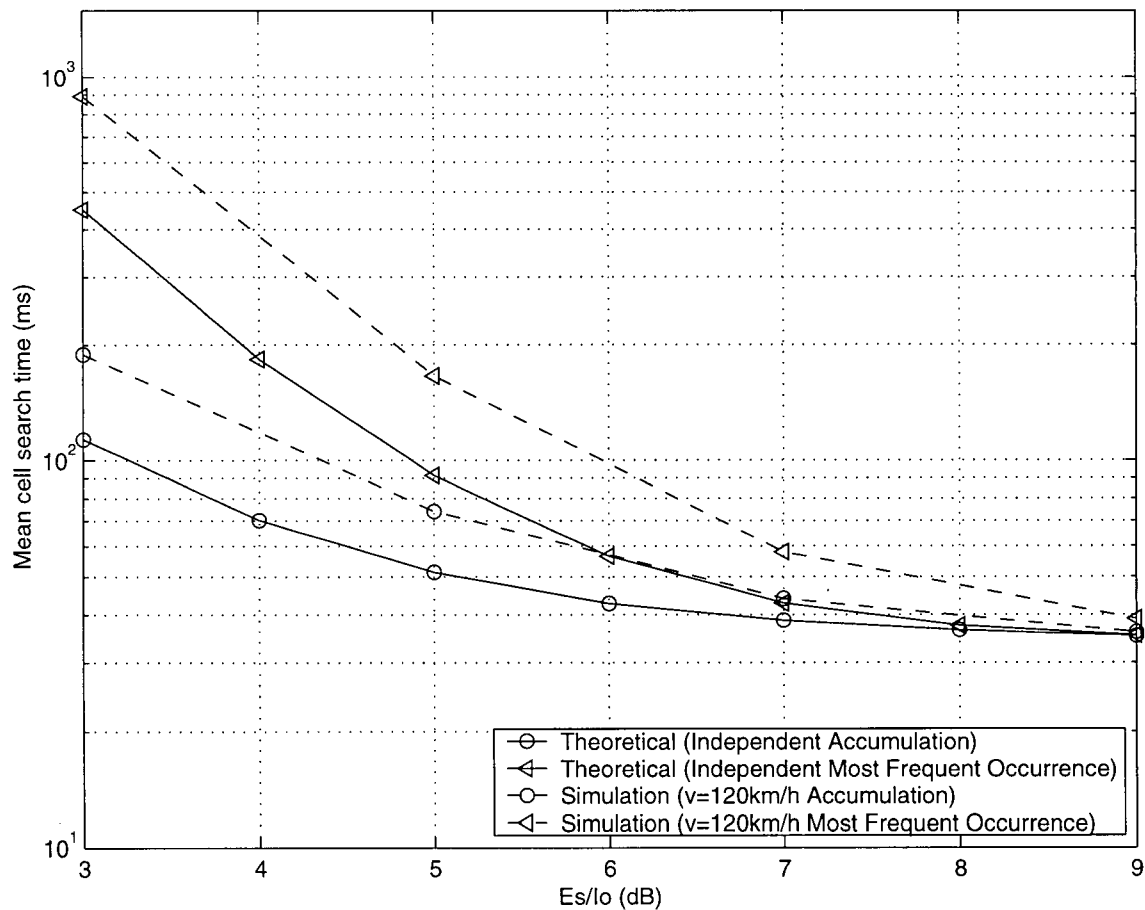


Figure 4.12 Mean cell search time under independent Ricean channel

In Figure 4.13, the theoretical results for the overall mean cell search time are presented assuming block Ricean fading. Also shown are simulation results at a vehicular speed of 3 km/h.

It can be seen that for the mean cell search time of 100 ms, the cell search algorithm using the accumulation technique has about 2.5 dB gain over the most frequent occurrence scheme.

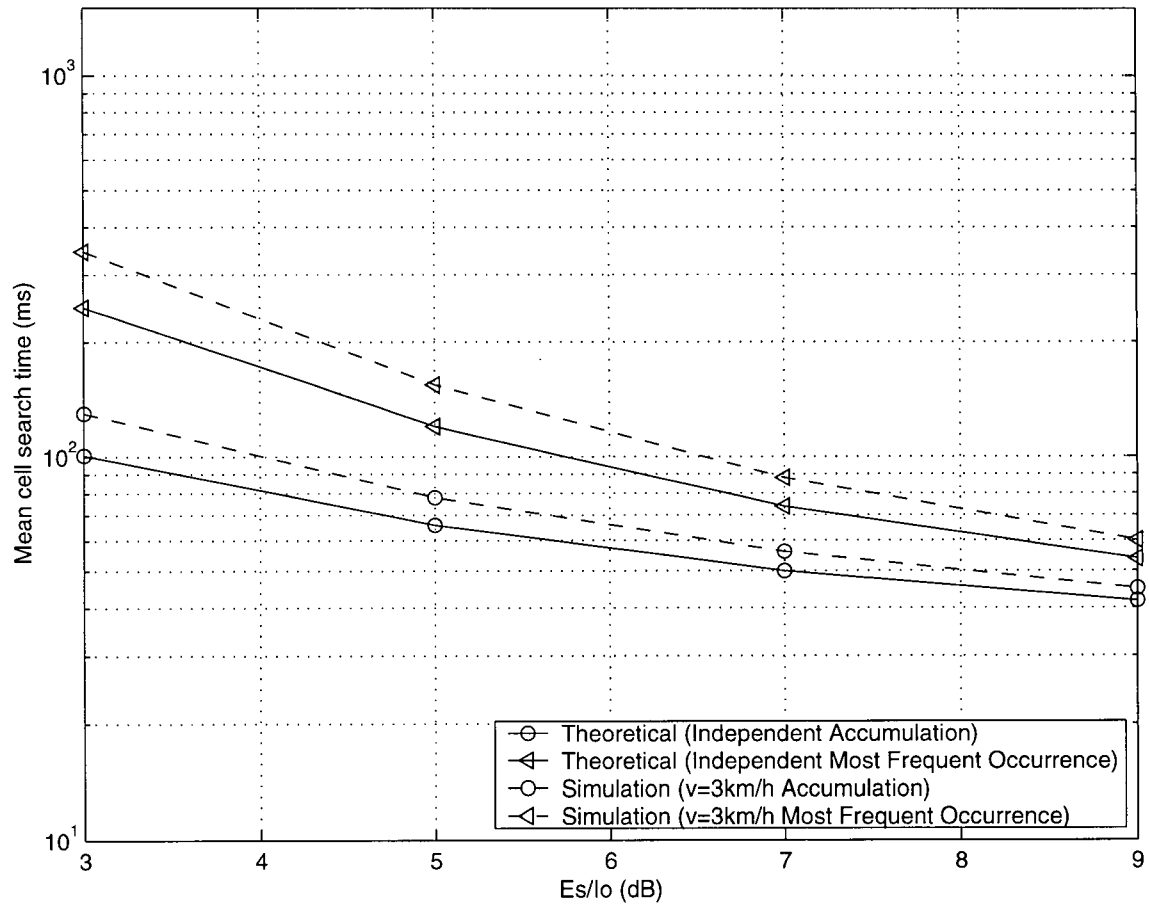


Figure 4.13 Mean cell search time under block Ricean channel

As observed in Figures 4.12 and 4.13, the mean cell search time in Ricean fading is less than that in Rayleigh fading. The improvement in Ricean fading vary from a few millisecond when  $E_s/I_0 = 9$  dB to a few hundred milliseconds when  $E_s/I_0 = 3$  dB.

## Chapter 5 Conclusion

### 5.1 Main Contributions of the Thesis

The goal of this thesis is to provide theoretical models for the detection probability for each of the 3 stages of the fast cell search algorithm and for estimating the average overall cell search time.

In this thesis, two slot synchronization methods were considered: the accumulation method and the most frequent occurrence method. It is shown that the accumulation method out-performs the most frequent occurrence method. For  $p_d^{(1)} = 0.5$ , there is about 3.5 - 4 dB gain for the accumulation technique at high vehicular speeds, e.g. 120 km/h. At low vehicular speeds, e.g. 3 km/h, the gain increases to about 4.5 - 5 dB.

Two idealized channel conditions, independent fading and block fading, were assumed in the analysis. At higher signal to interference ratios, the performance under independent fading conditions is better but degrades more rapidly as the channel condition deteriorates. A theoretical model for stage 2 is introduced in this thesis. The stage 2 probability of detection under independent fading condition is better when  $E_s/I_0$  is high, but degrades more rapidly when channel condition deteriorates.

Both Rayleigh and Ricean fading channels are used in the analysis. As expected, it is found that the probability of detection for all three stages in Ricean fading with 50% of the power in the line-of-sight path is higher than that in Rayleigh fading. The improvement in Ricean fading is about 0.5 dB for stage 1 and stage 2 and about 1 dB for stage 3.



It is also observed that the average overall cell search time is less when the accumulation method is used in stage 1, which agrees with the fact that in stage 1 the probability of detection using the accumulation method is higher than that using the most frequent occurrence method. For the mean cell search time of 100 ms, the cell search algorithm using the accumulation technique has about 1.5 dB gain over the most frequent occurrence scheme at high vehicular speeds, e.g. 120 km/h. At low vehicular speeds, e.g. 3 km/h, the gain for the accumulation technique increases to about 2.5 dB. It can be seen that the mean cell search time is less under independent fading when  $E_s/I_0$  is high, but increases more rapidly when  $E_s/I_0$  drops below 5 dB. As expected, the mean cell search time in Ricean fading is less than that in Rayleigh fading. The improvement in Ricean fading vary from a few millisecond when  $E_s/I_0 = 9$  dB to a few hundred milliseconds when  $E_s/I_0 = 3$  dB .

Simulations were also performed using SPW<sup>TM</sup>. Simulation results for a vehicular speed of 120 km/h are compared with the analysis results assuming independent fading. Because the independent fading assumption is not closely satisfied, there is a significant difference between the analysis and simulation results. Simulation results for a vehicular speed of 3 km/h agree closely with the analysis results assuming block fading.

## 5.2 Future Work

- The theoretical analysis results assuming independent fading does not closely match the simulation results at high vehicular speeds, e.g. 120 km/h. A better theoretical model which can accurately model such situations would be useful.

- The performance sensitivity of the cell search algorithm with imperfect sampling should be investigated.
- A threshold scheme could be implemented so that when the threshold in a certain stage is not met, that stage can be repeated without suffering the penalty of re-initializing the whole synchronization procedure.
- The effect of a frequency selective channel on the performance of the fast cell search algorithm should be investigated.

## **Glossary**

### **Acronyms**

3G - Third Generation

3GPP - Third Generation Partnership Project

BCH - Broadcast Channel

CDF - Cumulative Distribution Function

CDG - CDMA Development Group

CDMA - Code Division Multiple Access

CPICH - Common Pilot Channel

EDGE - Enhanced Data rates for GSM Evolution

ETSI - European Telecommunications Standardization Institute

FIR - Finite Impulse Response

GPRS - General Packet Radio Service

GPS - Global Positioning System

GSM - Global System for Mobile Communications

i. i. d. - independent, identical distributed

IMT - International Mobile Telecommunications

ITU - International Telecommunication Union

kbps - kilobits per second

ksym - kilosymbols

MAI - Multiple Access Interference

Mbps - Mega bits per second

MS - Mobile Station

OCNS - Orthogonal Channel Noise Simulator

OVSF - Orthogonal Variable Spreading Factor

P-CCPCH - Primary Common Control Physical Channel

PDC - Personal Digital Cellular

pdf - Probability Density Function

PSC - Primary Synchronization Code

P-SCH - Primary Synchronization Channel

QPSK - Quadrature Phase Shift Keying

TIA - Telecommunications Industry Association

SF - Spreading Factor

SPW<sup>TM</sup> - Signal Processing Worksystem

SRRC - Square Root Raised Cosine

SSC - Secondary Synchronization Code

S-SCH - Secondary Synchronization Channel

UTRAN - Universal Terrestrial Radio Access Network

W-CDMA - Wideband CDMA

### Notations

$C_{256,1}$  - Orthogonal Variable Spreading Factor code

$S_{dl,n}$  -  $n^{th}$  complex scrambling code sequence

$C_{psc}$  - primary synchronization code

$x$  - first generator polynomial used to generate a segment of a set of Gold codes

$y$  - second generator polynomial used to generate a segment of a set of Gold codes

$z_n$  -  $n^{th}$  Gold code sequence

$x(i)$  -  $i^{th}$  symbol of the sequence  $x$

$y(i)$  -  $i^{th}$  symbol of the sequence  $y$

$z_n(i)$  -  $i^{th}$  symbol of the sequence  $z_n$

$Z_n$  - real valued code sequence transformed from  $z_n$

$C_{ssc,k}$  -  $k^{th}$  secondary synchronization code

$N_1$  - number of slot durations accumulated in stage 1

$N_2$  - number of slot durations accumulated in stage 2

$N_3$  - number of slot durations accumulated in stage 3

$u$  - possible chip boundary locations of hypotheses in stage 1

$Y_1(u)$  - output of the correlator for the  $u^{th}$  hypotheses in stage 1

$v$  - possible SSC hypotheses in stage 2

$Y_2(v)$  - output of the correlator for the  $v^{th}$  hypotheses in stage 2

$w$  - possible scrambling code hypotheses in stage 3

$Y_3(w)$  - output of the correlator for the  $w^{th}$  hypotheses in stage 3

$y_i$  - received complex samples

$X_i$  - signal components at the correlator output at the  $i^{th}$  slot duration

$n_i^u$  - background multiple access interference (MAI) plus noise

$E_{s,PSCH}$  - average symbol energy for the P-SCH

$E_{s,SSCH}$  - average symbol energy for the S-SCH

$E_{s,CPICH}$  - average symbol energy for the CPICH

$I_0$  - background noise plus MAI variance

$F_N(\tau)$  - complementary cumulative distribution function of a  $\chi^2$  random variable with  $2N$  degrees of freedom

$p_{Y(0)}(\tau)$  - pdf of  $Y(0)$

$P_{Y(0)||X|^2=x}(\tau)$  - pdf of  $Y(0)$  given  $|X|^2 = x$

$p_{d_{slot}}^{(1)}$  - probability of detection for stage 1 when only one slot is observed

$p_d^{(1)}$  - probability of selecting the correct chip location as the estimate of the slot boundary  
in stage 1

$p_{d_{SSC}}^{(2)}$  - probability of correctly detecting SSC in stage 2

$p_d^{(2)}$  - probability of choosing the correct Frame SYNC sequence and its cyclic shift in  
stage 2

$p_{d||X|^2=x}^{(2)}$  - probability of detection for stage 2 given  $|X|^2 = x$

$p_{d_{SSC}||X|^2=x}^{(2)}$  - probability of correctly detecting SSC given  $|X|^2 = x$  in stage 2

$p_d^{(3)}$  - probability of choosing the correct scrambling code in stage 3

$T_1$  - duration of the first stage

$T_2$  - duration of the second stage

$T_3$  - duration of the third stage

$T_{pen}$  - penalty time

$p$  - probability of cell search success

$E[T]$  - mean cell search time



$\sigma_{noise}^2$  - noise variance

$I_{oc}$  - inter-cell interference level

$m$  - mean of the received signal in Ricean fading

$\sigma^2$  - identical variance of the received signal in Ricean fading

## References

- [1] P. Chaudhury, W. Mohr, and S. Onoe, "The 3GPP proposal for IMT-2000", *IEEE Communications Magazine*, pp. 72-81, Dec. 1999.
- [2] "CDMA2000 and 3GPP W-CDMA basics", *Wireless Technology Seminar*, Agilent Technologies, pp. 67-96, Burnaby, Canada, Dec. 2001.
- [3] E. Dahlman, B. Gudmundson, M. Nilsson, and J. Skold, "UMTS/IMT-2000 based on Wide-band CDMA", *IEEE Communications Magazine*, vol. 36, no. 9, pp. 70-80, Sept. 1998.
- [4] K. Higuchi, Y. Hanada, M. Sawahashi, and F. Adachi, "Experimental evaluation of 3-step cell search method in W-CDMA mobile radio", *IEEE 51st Vehicular Technology Conference*, pp. 303-307, Tokyo, Japan, 2000.
- [5] K. Higuchi, M. Sawahashi, and F. Adachi, "Fast cell search algorithm in DS-SS-SSMA mobile radio using long spreading codes", *IEEE 47th Vehicular Technology Conference*, vol. 3, pp. 1430-1434, Phoenix, AZ, 1997.
- [6] H. S. Lee, H. M. Pyo, and D. I. Kim, "Cell search scheme using I/Q multiplexed code assignment in asynchronous WCDMA system", *IEEE 49th Vehicular Technology Conference*, vol. 2, pp. 1560-1564, Houston, TX, 1999.
- [7] I. G. Kim, K. Kim, and B. W. Lim, "A fast cell search algorithm for inter-cell asynchronous W-CDMA system using code hopping method", *IEEE Global Telecommunication Conference*, vol. 3, pp. 1373-1377, Sydney, Australia, 1998.
- [8] J. H. Choi, N. M. Kim, and S. Y. Park, "A fast cell search algorithm using code block CPM in Asynchronous W-CDMA systems", *IEEE 52nd Vehicular Technology Conference*, vol. 1, pp. 280-285, Boston, MA, 2000.
- [9] 3rd Generation Partnership Project; Technical Specification Group Radio Access Network; Physical Channels and Mapping of Transport Channels onto Physical Channels (FDD), 3G TS25.211, Dec. 2001.
- [10] 3rd Generation Partnership Project; Technical Specification Group Radio Access Network; Spreading and Modulation (FDD), 3G TS25.213, Mar. 2000.
- [11] S. Kourtis, "The initial synchronization procedure in UMTS W-CDMA", *IEEE 5th Conference in Multiaccess, Mobility and Teletraffic*, pp. 97-106, Venice, Italy, October 1999.
- [12] H. Wang, Z. Chen, and M. Sundelin, "The impact of cell search on system performance in WCDMA", *IEEE 51st Vehicular Technology Conference*, vol. 2, pp. 1425-1429, Tokyo, Japan, 2000.

- [13] H. Olofsson, M. Sundelin, M. Edvardsson, and E. Dahlman, "Cell search performance in UTRA", *IEEE 50th Vehicular Technology Conference*, vol. 2, pp. 934-938, Amsterdam, The Netherlands, 1999.
- [14] S. Kourtis, "Investigation of the mobile terminal optimum operating point in UMTS-FDD initial cell search procedure", *IEEE 11th International PIMRC 2000*, vol. 1, pp. 348-352, London, England, 2000.
- [15] A. J. Viterbi, *CDMA Principles of Spread Spectrum Communication*, Addison Wesley, 1995.
- [16] J. G. Proakis, *Digital Communications*, 2nd edition, New York, McGraw-Hill, 1989.
- [17] S. Sriram, and S. Hosur, "An analysis of the 3-stage search process in W-CDMA", *IEEE 52nd Vehicular Technology Conference*, vol. 6, pp. 2672-2679, Boston, MA, 2000.
- [18] J. L. Devore, *Probability and Statistics for Engineering and the Sciences*, 3rd edition, Brooks/Cole Publishing Company, 1991.
- [19] T. S. Rappaport, *Wireless Communications, Principles and Practice*, Prentice Hall, 1999.

## Appendix A Allocation of SSCs for secondary SCH [10]

scrambling code group	slot number														
	#0	#1	#2	#3	#4	#5	#6	#7	#8	#9	#10	#11	#12	#13	#14
Group 0	1	1	2	8	9	10	15	8	10	16	2	7	15	7	16
Group 1	1	1	5	16	7	3	14	16	3	10	5	12	14	12	10
Group 2	1	2	1	15	5	5	12	16	6	11	2	16	11	15	12
Group 3	1	2	3	1	8	6	5	2	5	8	4	4	6	3	7
Group 4	1	2	16	6	6	11	15	5	12	1	15	12	16	11	2
Group 5	1	3	4	7	4	1	5	5	3	6	2	8	7	6	8
Group 6	1	4	11	3	4	10	9	2	11	2	10	12	12	9	3
Group 7	1	5	6	6	14	9	10	2	13	9	2	5	14	1	13
Group 8	1	6	10	10	4	11	7	13	16	11	13	6	4	1	16
Group 9	1	6	13	2	14	2	6	5	5	13	10	9	1	14	10
Group 10	1	7	8	5	7	2	4	3	8	3	2	6	6	4	5
Group 11	1	7	10	9	16	7	9	15	1	8	16	8	15	2	2
Group 12	1	8	12	9	9	4	13	16	5	1	13	5	12	4	8
Group 13	1	8	14	10	14	1	15	15	8	5	11	4	10	5	4
Group 14	1	9	2	15	15	16	10	7	8	1	10	8	2	16	9
Group 15	1	9	15	6	16	2	13	14	10	11	7	4	5	12	3
Group 16	1	10	9	11	15	7	6	4	16	5	2	12	13	3	4
Group 17	1	11	14	4	13	2	9	10	12	16	8	5	3	15	6
Group 18	1	12	12	13	14	7	2	8	14	2	1	13	11	8	11
Group 19	1	12	15	5	4	14	3	16	7	8	6	2	10	11	13
Group 20	1	15	4	3	7	6	10	13	12	5	14	16	8	2	11
Group 21	1	16	3	12	11	9	13	5	8	2	14	7	4	10	15
Group 22	2	2	5	10	16	11	3	10	11	8	5	13	3	13	8
Group 23	2	2	12	3	15	5	8	3	5	14	12	9	8	9	14
Group 24	2	3	6	16	12	16	3	13	13	6	7	9	2	12	7
Group 25	2	3	8	2	9	15	14	3	14	9	5	5	15	8	12
Group 26	2	4	7	9	5	4	9	11	2	14	5	14	11	16	16
Group 27	2	4	13	12	12	7	15	10	5	2	15	5	13	7	4
Group 28	2	5	9	9	3	12	8	14	15	12	14	5	3	2	15
Group 29	2	5	11	7	2	11	9	4	16	7	16	9	14	14	4
Group 30	2	6	2	13	3	3	12	9	7	16	6	9	16	13	12
Group 31	2	6	9	7	7	16	13	3	12	2	13	12	9	16	6

Table A.1 Allocation of SSCs for secondary SCH [10]

scrambling code group	slot number														
	#0	#1	#2	#3	#4	#5	#6	#7	#8	#9	#10	#11	#12	#13	#14
Group 32	2	7	12	15	2	12	4	10	13	15	13	4	5	5	10
Group 33	2	7	14	16	5	9	2	9	16	11	11	5	7	4	14
Group 34	2	8	5	12	5	2	14	14	8	15	3	9	12	15	9
Group 35	2	9	13	4	2	13	8	11	6	4	6	8	15	15	11
Group 36	2	10	3	2	13	16	8	10	8	13	11	11	16	3	5
Group 37	2	11	15	3	11	6	14	10	15	10	6	7	7	14	3
Group 38	2	16	4	5	16	14	7	11	4	11	14	9	9	7	5
Group 39	3	3	4	6	11	12	13	6	12	14	4	5	13	5	14
Group 40	3	3	6	5	16	9	15	5	9	10	6	4	15	4	10
Group 41	3	4	5	14	4	6	12	13	5	13	6	11	11	12	14
Group 42	3	4	9	16	10	4	16	15	3	5	10	5	15	6	6
Group 43	3	4	16	10	5	10	4	9	9	16	15	6	3	5	15
Group 44	3	5	12	11	14	5	11	13	3	6	14	6	13	4	4
Group 45	3	6	4	10	6	5	9	15	4	15	5	16	16	9	10
Group 46	3	7	8	8	16	11	12	4	15	11	4	7	16	3	15
Group 47	3	7	16	11	4	15	3	15	11	12	12	4	7	8	16
Group 48	3	8	7	15	4	8	15	12	3	16	4	16	12	11	11
Group 49	3	8	15	4	16	4	8	7	7	15	12	11	3	16	2
Group 50	3	10	10	15	16	5	4	6	16	4	3	15	9	6	9
Group 51	3	13	11	5	4	12	4	11	6	6	5	3	14	13	12
Group 52	3	14	7	9	14	10	13	8	7	8	10	4	4	13	9
Group 53	5	5	8	14	16	13	6	14	13	7	8	15	6	15	7
Group 54	5	6	11	7	10	8	5	8	7	12	12	10	6	9	11
Group 55	5	6	13	8	13	5	7	7	6	16	14	15	8	16	15
Group 56	5	7	9	10	7	11	6	12	9	12	11	8	8	6	10
Group 57	5	9	6	8	10	9	8	12	5	11	10	11	12	7	7
Group 58	5	10	10	12	8	11	9	7	8	9	5	12	6	7	6
Group 59	5	10	12	6	5	12	8	9	7	6	7	8	11	11	9
Group 60	5	13	15	15	14	8	6	7	16	8	7	13	14	5	16
Group 61	9	10	13	10	11	15	15	9	16	12	14	13	16	14	11
Group 62	9	11	12	15	12	9	13	13	11	14	10	16	15	14	16
Group 63	9	12	10	15	13	14	9	14	15	11	11	13	12	16	10

Table A.1 Allocation of SSCs for secondary SCH [10]